AD-A162 137 DEVELOPMENTS IN MODELLING THE USE OF INFRARED OFFBOARD COUNTERMEASURES IN AN INFRARED ANTI-SHIP MISSILE SCENARIO(U) NAVAL POSTGRADUATE SCHOOL MONTEREY CA 1/2

UNCLASSIFIED V D REED SEP 85 F/G 17/4 NL

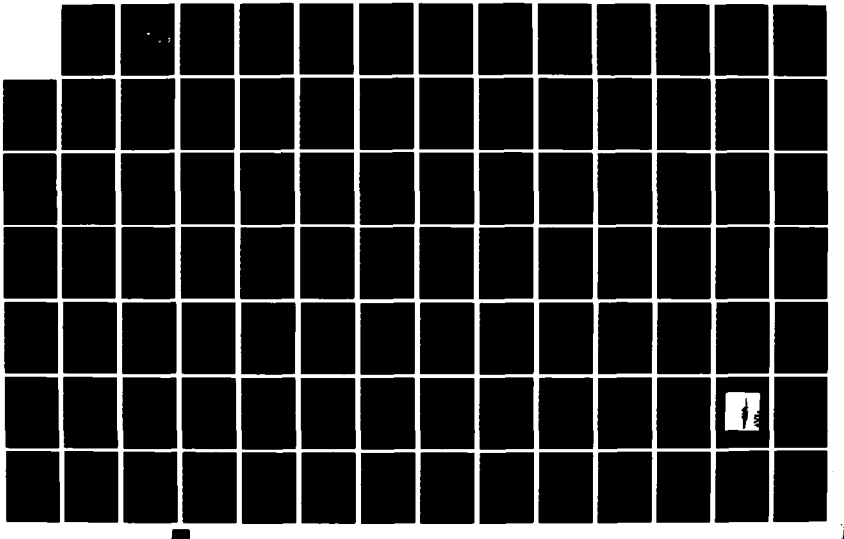

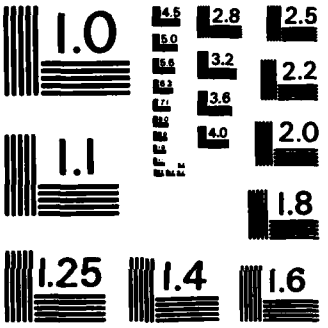

NAVAL POSTGRADUATE SCHOOL
Monterey, California

THESIS

DEVELOPMENTS IN MODELLING THE USE OF INFRARED OFFBOARD COUNTERMEASURES IN AN INFRARED ANTI-SHIP MISSILE SCENARIO

by

Vernon Daniel Reed

September 1985

Thesis advisor: A. W. Cooper

Approved for public release; distribution is unlimited.

SECURITY CLASSIFICATION OF THIS PAGE (When Data Entered)

REPORT DOCUMENTATION PAGE		READ INSTRUCTIONS BEFORE COMPLETING FORM
1. REPORT NUMBER	2. GOVT ACCESSION NO. AD-A162 137	3. RECIPIENT'S CATALOG NUMBER.
4. TITLE (and Subtitle) Developments in Modelling the Use of Infrared Offboard Countermeasures in an Infrared Anti-Ship Missile Scenario		5. TYPE OF REPORT & PERIOD COVERED Master's thesis; September 1985
		6. PERFORMING ORG. REPORT NUMBER
7. AUTHOR(s) Vernon Daniel Reed		8. CONTRACT OR GRANT NUMBER(s)
9. PERFORMING ORGANIZATION NAME AND ADDRESS Naval Postgraduate School Monterey, California 93943-5100		10. PROGRAM ELEMENT, PROJECT, TASK AREA & WORK UNIT NUMBERS
11. CONTROLLING OFFICE NAME AND ADDRESS Naval Postgraduate School Monterey, California 93943-5100		12. REPORT DATE September 1985
		13. NUMBER OF PAGES 105
14. MONITORING AGENCY NAME & ADDRESS(if different from Controlling Office)		15. SECURITY CLASS. (of this report)
		15a. DECLASSIFICATION/DOWNGRADING SCHEDULE

16. DISTRIBUTION STATEMENT (of this Report)

Approved for public release; distribution is unlimited.

17. DISTRIBUTION STATEMENT (of the abstract entered in Block 20, if different from Report)

18. SUPPLEMENTARY NOTES

The research described in this thesis was carried out under sponsorship of COMSPAWARSYSCOM, (PDE107-5), under documents N0003985WRDJ181, N0003985WRDJ621, and N0003985WRDJ903. REWSON support of this program is gratefully acknowledged.

19. KEY WORDS (Continue on reverse side if necessary and identify by block number)

Atmospheric transmittance, infrared, offboard countermeasures, LOWTRAN, modelling, simulation

20. ABSTRACT (Continue on reverse side if necessary and identify by block number)

This work deals with the evolution of a FORTRAN simulation written by Naval Research Laboratory which is used to evaluate the effectiveness of deploying ship-launched infrared decoys to counter the anti-ship infrared seeking missile threat. Although the model (referred to as the Stochastic Infrared Engagement Model - SIREM) possesses extensive analytical capability and flexibility, refinements are desired to more accurately emulate atmospheric effects on the acquisition process. Methods are derived

DD FORM 1 JAN 73 1473 EDITION OF 1 NOV 65 IS OBSOLETE

S N 0102-LF-014-6601

SECURITY CLASSIFICATION OF THIS PAGE (When Data Entered)

Block 20 Contd.

herein to calculate atmospheric transmittance as a function of range using an accurate, LOWTRAN-based empirical formula.

Basic seeker discrimination techniques are addressed which may be incorporated into SIREM or other simulations for future missile-versus-decoy evaluations; and some ideas are presented which may prove valuable in decoy enhancement to subjugate the discriminating seeker.

Approved for public release; distribution is unlimited.

Developments in Modelling the Use of Infrared Offboard Countermeasures in an Infrared Anti-Ship Missile Scenario

by

Vernon Daniel Reed
Lieutenant, United States Navy
B.S.E.E., University of Missouri, 1978

Submitted in partial fulfillment of the requirements for the degree of

MASTER OF SCIENCE IN SYSTEMS ENGINEERING
ELECTRONIC WARFARE

from the

NAVAL POSTGRADUATE SCHOOL
September 1985

Author: Vernon D Reed
Vernon Daniel Reed

Approved by: A.W. Cooper
Alfred W. Cooper, Thesis Advisor

Harold Titus
Harold Titus, Second Reader

John M. Boulder
John M. Bouldry, Chairman, Electronic Warfare Academic Group

David A. Schrady
David A. Schrady, Academic Dean

ABSTRACT

This work deals with the evolution of a FORTRAN simulation written by Naval Research Laboratory which is used to evaluate the effectiveness of deploying ship-launched infrared decoys to counter the anti-ship infrared seeking missile threat. Although the model (referred to as the Stochastic Infrared Engagement Model - SIREM) possesses extensive analytical capability and flexibility, refinements are desired to more accurately emulate atmospheric effects on the acquisition process. Methods are derived herein to calculate atmospheric transmittance as a function of range using an accurate, LOWTRAN-based empirical formula.

Basic seeker discrimination techniques are addressed which may be incorporated into SIREM or other simulations for future missile-versus-decoy evaluations; and some ideas are presented which may prove valuable in decoy enhancement to subjugate the discriminating seeker.

TABLE OF CONTENTS

I. INTRODUCTION ---------- 1

II. ATMOSPHERIC ENVIRONMENT ---------- 6

III. ENGAGEMENT SCENARIO ---------- 15

IV. ATMOSPHERIC MODELLING ---------- 23

A. LOWTRAN ---------- 24

1. Modelling Example ---------- 39

a. Empirical Equation for Extinction --- 45

V. STOCHASTIC INFRARED ENGAGEMENT MODEL (SIREM) ---- 55

VI. IR SEEKER SYSTEMS AND COUNTERMEASURES ---------- 62

A. SCANNING AND STARING SYSTEMS ---------- 62

1. Filtering for Discrimination ---------- 71

APPENDIX A LOWTRAN AND EMPIRICAL TRANSMITTANCE TABLES - 79

APPENDIX B COMPUTER CODING FOR TRANSMITTANCE MODELLING - 95

LIST OF REFERENCES ---------- 98

BIBLIOGRAPHY ---------- 99

INITIAL DISTRIBUTION LIST ---------- 100

I. INTRODUCTION

With the advent of the missile era has come a revolution in naval warfare methods. The problem of contending with "smart" weapons has given a whole new meaning to both offense and defense alike. These missiles may employ a variety of acquisition hardware. Some will be passive, some active, and some both.

Particular problems arise when missiles use passive acquisition methods. Passive sensors radiate nothing and are therefore invisible to conventional electronic support measures (ESM). Furthermore, their small size allows them to reflect only meager amounts of radar energy, which further reduces reaction and countermeasure employment time of the ship. The countermeasures may be in the form of onboard or offboard weapons systems or deception devices. The cost versus effectiveness of onboard close-in weapon systems has been a driving factor in the Navy's desire to analyze the employment of offboard expendable seduction and distraction devices as a relatively inexpensive alternative.

Here we will restrict our studies to the passive infrared seeking missile problem, although concurrent analysis is being conducted to contend with the active RF missile seekers.

To reduce radically the cost of development of offboard device characteristics and deployment tactics, a computer simulation has been constructed to assist in the analysis process. This modelling program is appropriately named the "Stochastic Infrared Engagement Model - SIREM". It originated at Naval Research Laboratory in Washington, D.C., and was transported to the Naval Postgraduate School in Monterey, CA to assist in the analysis of the use of infrared decoys as a counter to the passive seeker problem. It is designed to imitate the typical cruise-missile versus ship engagement scenario and to establish measures of effectiveness (MOEs) for both 1) decoy characteristics, and 2) deployment tactics. Therein lies the basis for continuing verification and upgrades to the model so that it remains capable of accurate evaluation of the hardware at hand.

Most real-world systems are very complex. In order to model any system accurately, all factors which affect it must be represented in as accurate a fashion as possible. Weaknesses in representation should be identified and documented so that overconfidences in the output do not occur. Once documented, the weak areas of the model may be studied and reworked to increase the accuracy of the model.

This paper deals with the evolution of SIREM. By simulating each component of the engagement scenario in a realistic manner, the optimum decoy deployment schemes can

be obtained, combined with their RF counterparts, and algorithmically automated for deployment via computer in order to reduce chances of operator control errors. It can easily be seen here that it is not financially or logistically feasible to evaluate all scenarios in field tests using real ships and missiles, since the cost would be prohibitive.

Extensive conversion and review of the SIREM model was conducted to assist in its enhancement. Two specific areas of weakness were identified which require some attention. The first area of concern was a lack of atmospheric attenuation on the emitted IR signatures of the ship and/or decoys. The second regards the study of seeker head discrimination techniques and how to implement them based on data available. The emphasis in this paper revolves around finding a simple technique for calculating atmospheric transmittance throughout the path of an incoming infrared seeking missile which will accurately affect its probability of acquisition in the simulation environment. Two methods currently used in obtaining transmittance in a stochastic model such as SIREM involve either look-up tables which are either incomplete or inflexible, or incorporation of the LOWTRAN program as a subroutine. The second method is preferred since it is very flexible to observed atmospheric conditions; however, it requires an extension of 9000 lines of FORTRAN code along with the added input-output coding,

which serves only to calculate one value of atmospheric transmittance for each incremental range throughout the missile flight path. It was felt by the author that this was excessively wasteful of valuable computer time and memory requirements considering the model's current size of approximately 15,000 lines of code.

The intent was to devise a simpler scheme for finding as accurately as possible what the atmospheric transmittance would be for a given set of atmospheric conditions that would be easily incorporated into the incremental flight path of a missile and more accurately affect the seeker head acquisition probability.

To more fully understand the principle of atmospheric transmittance and its effects, one chapter is dedicated to explaining the basic principles of atmospheric transmittance. Once a good understanding of the principles of atmospheric transmittance has been gained by the reader, an introduction to the LOWTRAN program is performed, presenting its capabilities for prediction of transmittance. This will be followed by a simplistic approach for modeling atmospheric transmittance with very short computer coding schemes.

The closing chapters will be dedicated to more detailed explanation of the SIREM modelling program, followed by an introduction to possible discrimination techniques Since seeker discrimination adds to the problems surrouding the

use of offboard countermeasures, the subject of enhancing current decoy designs by taking advantage of certain natural phenomenon is addressed in the concluding chapter.

Future enhancements to SIREM to incorporate both transmittance and discrimination techniques are the object of this work and concurrent work by Naval Research personnel. These enhancements are intended to more accurately reflect the acquisition probability of the seekers being modelled so that refinements to the design and deployment of offboard countermeasures are possible.

II. ATMOSPHERIC ENVIRONMENT

This chapter is dedicated to reviewing the principles of atmospheric propagation of infrared radiation, the causes of its variability, and tools available to predict how much is transmitted at various ranges and atmospheric conditions.

The atmosphere is comprised of numerous gasses - nitrogen, oxygen, water vapor, carbon dioxide, methane, carbon monoxide, and ozone to name the major components. Additionally there are numerous suspended particles distributed in various densities throughout the earth's atmosphere. The major constituents of the atmosphere are nitrogen, comprising 78%, and oxygen, which occupies 20% of the total volume. Water vapor makes up 1%, while carbon dioxide constitutes only 0.04% of the atmosphere. The transmission of infrared radiation through the atmosphere depends on the meteorological conditions, and hence varies with weather conditions and altitude. Only an approximate result can be gained through the theoretical study of the principles of atmospheric attenuation since no definitive conclusions can be made. The base of knowledge regarding atmospheric attenuation and the associated formulae comes principally from empirical means or approximations.

The primary factor in absorption in the infrared spectrum is water vapor. The wide variations in concentration and distribution of water vapor in the atmosphere are the primary reasons for the variance in absorption levels from one meteorological profile to the next. Although carbon dioxide comprises only 4/100 percent volume of the atmosphere, it is second in importance as an attenuator of infrared radiation, as well as being more uniformly distributed than water vapor.

There are three major factors which contribute to the attenuation of infrared radiation: Extinction, or the loss of energy resulting from the interaction of the beam with the various absorbing or scattering constituents contained in the atmosphere; Refraction, or the bending of light rays due to the refractive index gradients of the atmosphere, and Scintillation, or the distortion of the optical beam due to small scale turbulence. Refraction will not be discussed heavily here since it will be apparent later that it may serve only to extend the optical horizon of infrared seeking missiles, but have little affect on the simulation discussed herein. Extinction represents the combined effects of the scattering of radiation into or out of the beam due to aerosols and air molecules present in the beam path, and absorption caused by the direct transfer of energy from radiation generated by the source to the vibrational or

rotational kinetic energy of the molecules and aerosols. This is illustrated in the following diagram.

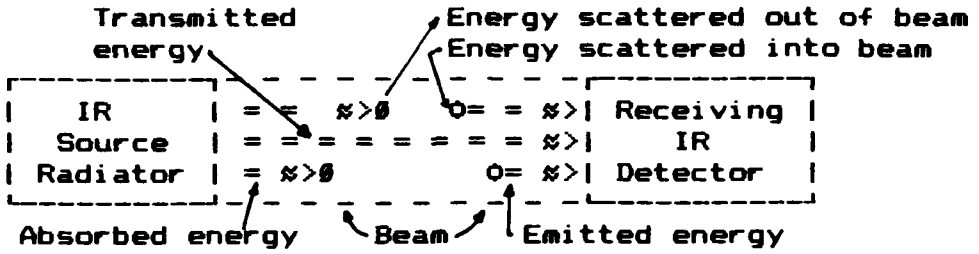

Figure 2-1. Causes of extinction

The attenuation or extinction of electromagnetic radiation is described by the Lambert-Beer-Bouguer Law

$$I = I_o \epsilon^{-\beta R} \qquad \text{(Eq. 2.1)}$$

where I is the attenuated radiation, I_o is the source radiation, β is the attenuation coefficient, and R is the path length. The extinction is caused by absorption and scattering by molecules and aerosols. They contribute linearly to the the total extinction as follows:

$$\beta = \beta_{MA} + \beta_{MS} + \beta_{AA} + \beta_{AS} \qquad \text{(Eq. 2.2)}$$

where β_{MA}= molecular absorption by water vapor, ozone, etc.

β_{MS}= molecular (Rayleigh) scattering

β_{AA}= aerosol absorption (dry particles neglected)

β_{AS}= aerosol (Mie) scattering

The importance of each of these effects depends on the wavelength of the electrooptic energy. The wavelength

dependencies exist because of the relative sizes of the responsible constituents (molecule or aerosol) and the energy states of the molecules (molecular absorption bands). The importance of the principal component of attenuation for the primary wave bands is given here.

TABLE 2.1. PRIMARY ATTENUATORS IN IR SPECTRUM

Wavelength Region (In micrometers)	Attenuation Coefficients In order of importance
Visible .4 - .7 micron	β_{MA}, β_{MS}
Near IR .7 - 2 micron	β_{AS} (β_{MA} for some wavelengths)
Mid IR 3 - 5 micron	β_{MA} (H_2O), β_{AS}
Far IR 8 - 14 micron	β_{MA} (H_2O), β_{AS}

The aerosol relationship used to describe extinction is principally governed by the size (aerosol radius) of the particle and the wavelength of the incident energy as:

1) Rayleigh Scattering (where $r<<\lambda$ - molecule effects).
2) Mie Scattering (where $r \approx \lambda$ approximately).
3) Geometric Scattering (where $r>>\lambda$ - large particles).

An illustration of the scattering description is as shown here.

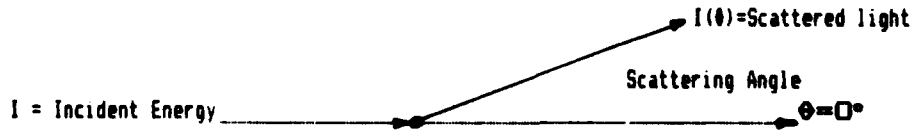

Figure 2-2. Scattering Geometry

The attenuation scattering cross-section for one particle of size r and wavelength λ is the integral of the scattering in all directions:

$$S = \int_{\text{Solid Angle}} I(\theta)\, d\Omega \qquad \text{(Eq. 2.3)}$$

Mie scattering is generally concentrated in the forward direction as follows.

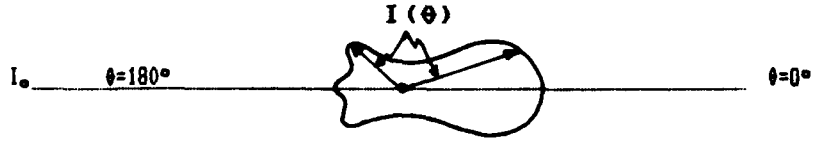

Figure 2-3. Mie Scattering

Note that a minimum occurs near the ±100° points and that a secondary peak occurs in the backward direction (back-scatter).

Rayleigh scattering is symetrical as shown.

Figure 2-4. Rayleigh Scattering

The scattering efficiency Q of a particle is given by the cross-section S (above) divided by the area of the particle.

$$Q = \frac{S}{\pi r^2} \qquad \text{(Eq. 2.4)}$$

For Rayleigh scattering Q is on the order of λ^{-4}, and based on the wavelength span present from the sun's radiation, is

the principal factor in the sky's blue appearance. Q is higher at the longer wavelengths. For geometric scattering Q ≈ 2.0. Only particles with radii between about 0.1 and 1.0 micrometers are effective in scattering light in the visible range. These particles are too small to rain out due to their low collection efficiency. This is why rain alone does not reduce haze and increase visibility. A change in the vertical temperature profile (such as the breaking up of an inversion layer by a frontal passage) does increase horizontal visibility through upward diffusion of the aerosols.

Because the scattering efficiency Q is a function of aerosol size and wavelength, scattering itself is a function of wavelength.

$$\beta_{As} \propto \lambda^{-\alpha} \qquad \text{(Eq. 2.5)}$$

Here α is the Angstrom coefficient, and varies generally from 0.5 to 2.0. This value may be as high as 4.0 for Rayleigh scattering. The scattering coefficients for various aerosol types are shown below.

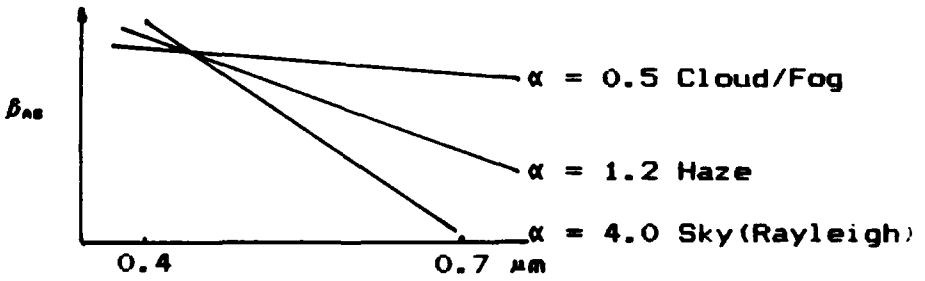

Figure 2-5 Scattering Coefficient

With this diagram we see that the wavelength dependence of scattering explains why the sky is blue, since the shorter wavelengths are scattered so much more. Likewise heavy haze can cause the red sunset effect since the longer wavelengths are not scattered out of the path. Note also how the cloud, fog, and haze coefficients carry over into the infrared region. We can expect these to be major factors in transmittance reduction there.

Scattering is also indirectly a function of relative humidity (RH) because as RH increases, the water molecules collect on a dry particle until enough of them are on the particle to cause it to go into a solution and form a droplet. This is called deliquescence. Since a solution droplet can grow in size much faster than a particle, the scattering increases rapidly with RH due to an aerosol rapidly changing its size distribution through growth of droplets. Typical scattering coefficient variations are shown below. These are presented as a ratio of the scattering coefficient for aerosols to the scattering coefficients for aerosols at 20% relative humidity as a function of relative humidity.

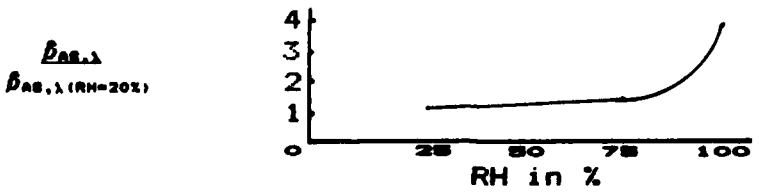

Figure 2-6 Scattering Coefficient Variation

Models of the aerosol distribution in the marine environment can be very complex because of the amount and size of the particles present in the marine environment. These are functions of particle generation at the sea surface and the vertical transport of the particles once they are suspended in the atmosphere.

Wind speed dependence on aerosol distribution in the maritime model is similar to that of continental models until the wind speed nears 14 knots. At 14 knots the aerosol concentration has increased by a factor of about 1.5 due to aerosol generation by the surface whitecaps which form at this wind speed. As the wind speed increases, the concentration may rise to a value of 10 to 100 times the calm atmospheric value near the surface, but decrease in concentration with altitude up to approximately 5 kilometers.

It can now be seen that the atmospheric conditions have a dramatic effect upon the extinction and absorption at various wavelengths. In this paper the interest lies primarily in the infrared region since this is where our model (SIREM) is designed to simulate target acquisitions. Hence it is good practice to become familiar with those factors which affect the systems being modeled. Incorporation of "real-world" occurrences is a vital part of systems modeling. Those models which use random (non-deterministic) methods to emulate a patterned parameter can

only be termed less than valid. They would serve useful for nothing more than gaming exercises since the answers could not be relied upon.

Since the SIREM model is designed to obtain measures of effectiveness of IR decoy deployment versus an IR seeking missile, those measures may only be obtained through realistic incorporation of the factors that affect the engagement. The primary intent of the following chapters is to define the scenario, present the principles of detection, and show how the LOWTRAN program can be used to develop a very compact and accurate method of incorporating atmospheric absorption into the acquisition process.

III. ENGAGEMENT SCENARIO

As with any detection method, whether RF, visible, or infrared, it is assumed that the target is either emitting or reflecting energy at some power density in the frequency band of the detector as in the scenario shown below.

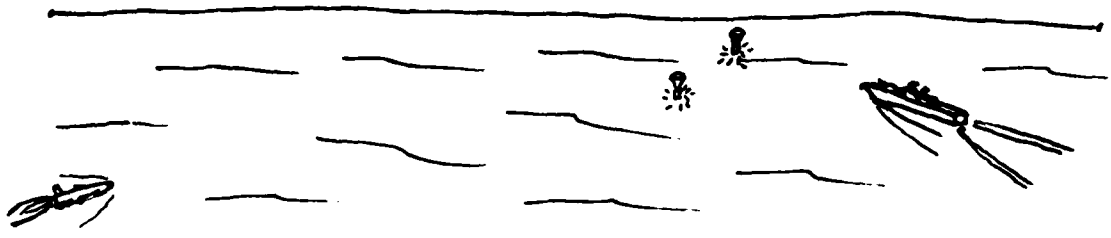

Figure 3-1. IR Missile Attack Scenario

From extended ranges this emission or reflection can be assumed to appear as a point source, however at closer ranges the physical size of the target must be expanded into a distributed source emitter, especially considering the typical optical magnification performed by the seeker. Since this document deals specifically with infrared emission and transmission, the case of target reflection will henceforth be disregarded.

The unit of measure given to the power emitted from the target is the radiant intensity (J), commonly stated in watts per steradian (solid angle). The target, assumed to be a point source, emits a source level radiation in

specific spectral bands. The radiant flux density of any wavelength across the continuum has a natural reduction in value based on the inverse square law with range from the ship (target) to the missile (receiving platform).

The detector in the seeker head is composed of a material which electrically (via photon energy) sensitive to incoming radiation across some defined frequency bandwidth inherent to the composition. This bandwidth is preferrably fairly narrow. If it is allowed to become excessively wide, the signal-to-noise ratio is reduced an unacceptable level of false alarm detections as discussed by Hudson [Ref. 2:ch. 12]. For this reason most detector systems have external spectral filters to narrow the bandwidth and eliminate these misdetections.

Based on the composition of the detector material each detector will have an optimum electrically active wavelength to which it is sensitive. As the incoming energy shifts in frequency to either side of the optimum, the electrical activity in the detector is reduced, creating some distribution which reflects the electrical activity, or molecular transition density as a function of wavelength. This relationship should be known in order to reflect any spikes in the sensitivity curve where certain energy bands may be particularly absorptive of incident energy. The

profile shown in Figure 3-2 is one which could be used in the typical simulation environment based on the above principles.

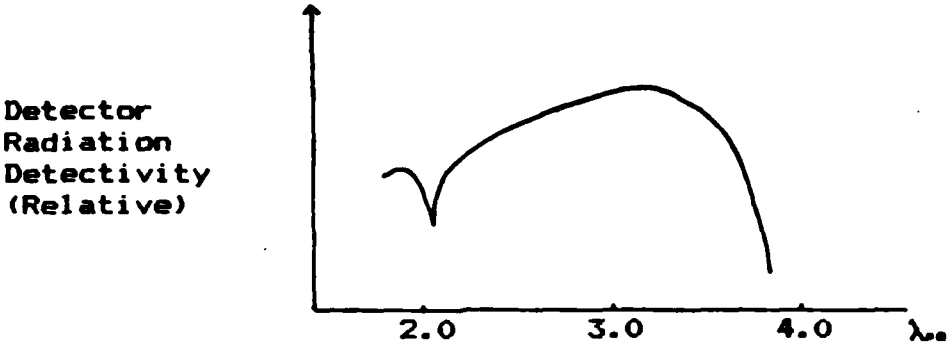

Figure 3-2.Detectivity over Bandwidth

The actual electrical bandwidth of a detector has three primary dependencies: first, the material from which it is constructed; second, the temperature at which it is operated; third, the physical area of the detector surface. The detectivity (D*) is the convenient measure categorizing a detector's operation within these parameters. It normalizes the "sensitivity" of various detectors to an electrical bandwidth of 1 Hz, and an area of 1 square centimeter, and is a convenient means for comparing the equivalent electrical response between detectors in circuits of different bandwidth. Shown in Figure 3-3 is a typical Lead Sulfide detector's D* characteristics taken from Hudson [Ref. 2:pp. 365].

Lead Sulfide (PbS)

Type: Photoconductive.

Element sizes available: From 0.01 × 0.01 to 25 × 25 mm. Rectangular elements from 0.01 mm wide. For arrays, minimum element spacing is 0.01 mm.

Temp. (°K)	Time constant (μsec)	Resistance (megohms)	ℛ (VW⁻¹)	D^* (peak) / D^* (500°K)
295	50–500	0.1–0.6	4×10^4	90
195	800–4000	3–6	3×10^5	25
77	500–3000	6–12	2×10^6	60

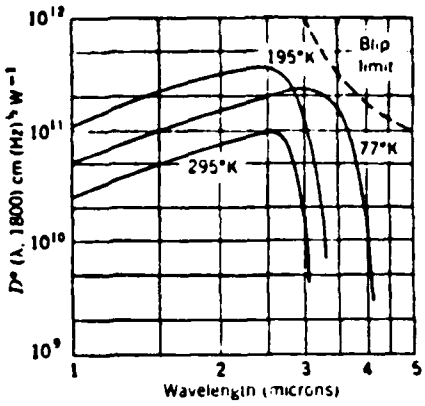

Figure 3-3. Detectivity versus Wavelength

The value of D* is dependent upon the temperature, wavelength and bias current applied. The low temperatures are required, as well as bias current, to maximize the system's signal-to-noise ratio.

The object of our simulation is to characterize the search and acquisition process as closely to actual as possible. To do this we must model the detection process (seeker), atmospheric effects, flight characteristics of the missile, and target (ship or decoy) signatures as closely as possible. Taking all factors into account, the maximum range of the detector must be calculated.

The spectral irradiance from a target (assumed distant in the field of view (FOV) is

$$H_\lambda = \frac{J_\lambda \, T_a(\lambda)}{R^2} \quad \text{in Watts/cm}^2 \qquad \text{(Eq. 3.1)}$$

where $\tau_a(\lambda)$ is the transmittance of the path, and the subject of following chapters. R is the distance from the seeker to the target.

The spectral radiant power into the detector is

$$P_\lambda = H_\lambda A_o \tau_o(\lambda) \qquad \text{in Watts} \qquad \text{(Eq. 3.2)}$$

where Ao is the area of the entrance aperature of the optics, and $\tau_o(\lambda)$ is the transmittance of the whole sensor system. $\tau_o(\lambda)$ is the product of the transfer functions for the detector and all external filter functions such as protective windows, lenses, reticles, and maskings.

The signal voltage from the detector is

$$V_s = P_\lambda \mathcal{R}(\lambda) \qquad \text{(Eq. 3.3)}$$

where $\mathcal{R}(\lambda)$ is the spectral responsivity of the detector.

Thus far the equations represent an infinitesimal spectral interval centered about some wavelength λ. Since there is a finite bandwidth to an actual system, this should be taken into account as shown in Hudson [Ref. 2:ch. 13]. Remember, however, that we are assuming "worst case" in the simulation process. So, by selecting the optimum detectivity wavelength of the particular detector, we have effectively maximized the range of detection for our seeker. This assumption may only be made if the seeker system being modelled has a relatively narrow spectral response due to

external filtering for a better signal-to-noise ratio. This is virtually always the case from design inception since the false alarm problem is critical here.

Further development of the equations above is performed by Hudson and leads to the Optical Trade-Off Equation:

$$R = [J\tau_A]^{1/2} \left[\frac{\pi D_o (NA) \tau_o}{2}\right]^{1/2} [D^*]^{1/2} \left[\frac{1}{(\omega \Delta f)^{1/2} (V_s/V_N)}\right]^{1/2} \quad \text{(Eq. 3.4)}$$

_1_/ ___2___/ _3_/ _____4_____/

1 - Target irradiance and atmospheric transmittance
2 - Optics parameters
3 - Detector characteristics
4 - System parameters and signal processing

where R = detection range.
D_o = diameter of entrance of aperture optics.
NA = numerical aperture [Ref. 2:ch. 5].
ω = instantaneous field of view of sensor.
Δf = frequency bandwidth in Hz.
V_s/V_N = signal to noise ratio [Ref. 2:pp. 419].

By breaking the equation into sections as shown above we see in the first term that reduction of target signature (ship) and enhancement of the decoy signature inband would shift the acquisition probability more toward the decoy. In the engagement process nothing can be done about the atmospheric transmittance, although it does have dramatic effects on the acquisition range. Knowing the parameters of the second, third and fourth term facilitates modelling various missile/seeker systems.

At ranges beyond the sensitivity of the seeker head, i.e. where incident energy is insufficient, detection probability would be zero. In addition to the inverse square law power loss, the atmospheric losses previously discussed must be taken into account in order to accurately determine detection probability. Since the detectivity of the seeker is independent of the atmospheric effects on the emitted signature, the resultant probability of detection would be the product of probability of detection assuming no atmospheric effects, and the atmospheric transmittance which varies from 0 to 1.

Few models if any actually emulate the signal integrating principle upon which most detectors depend for threshold detection. The scanning technique, whether serial or parallel, performs the temporal integral of the incoming energy across the "window function" which defines the acceptance bandwidth of the seeker. The seeker system's probability of detection curve-versus-wavelength is proportional to the detector's detectivity-versus-wavelength curve.

The present version of the SIREM model emulates a scanner type seeker with limited field of view typical of the ASMs previously discussed. This model is presently being upgraded to account for atmospheric losses over range. It will do so by assuming the "worst case" posture. By this, it is meant that at the optimum detector wavelength,

the model presently calculates probability of detection for incremental missile movements. This value is calculated as a "worst case" value for the ship based on the detectivity of the seeker and the maneuvering capability of the missile. By multiplying the probability of detection (assuming no losses) at each range increment by the corresponding transmittance value at that range, the target acquisition probability is more accurately represented. This is the case whether the acquired target is a decoy or the ship.

As an example assume that the transmittance has been calculated for a given atmospheric profile for the engagement scenario. The transmittance is then known at each increment of range. As the missile approaches its target the atmospheric transmittance increases approximately exponentially. If the probability of detection is calculated for the seeker system in each incremental movement performed by the simulation, the engagement scenario probability of detection for the missile would be the product of transmittance and original seeker acquisition probability generated by its own separate technique. Hence if the original P_d were 0.8, and the transmittance were 0.6, the total system probability of detection would then be 0.48.

IV. ATMOSPHERIC MODELLING

The previous chapters presented the principles of propogation of infrared radiation throughout the atmosphere and the factors which affect the acquisition process. This chapter will deal with an empirical approach to modelling the atmospheric transmittance using very accurate single equations once the conditions of visibility, range and wind speed are given.

Atmospheric transmittance losses for infrared radiation, not unlike radio frequency transmission losses, exhibit the characteristic $1/(\text{Range})^2$ loss factor as shown below.

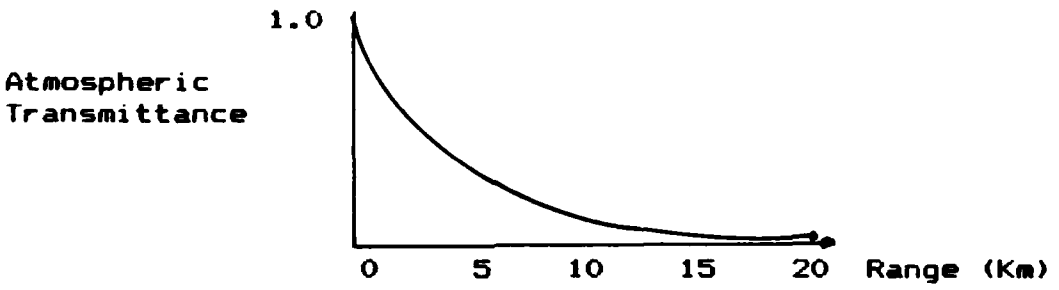

Figure 4-1. Transmittance versus Range.

An actual curve varies widely in its rate of transmission loss with range depending heavily upon the particular infrared wavelength in question, the amount and size of particulate matter in the air, the altitude(s), and weather conditions as discussed previously. The LOWTRAN program [Ref. 1] was developed to a large extent from empirical

observations and is used to predict atmospheric transmittance for any given set of conditions. The desired goal in the continuing development of the SIREM model was to find a simple technique for incorporating the calculation of atmospheric transmittance into the incremental range movements of a simulated incoming missile and its associated infrared seeker head in order to more accurately portray the probability of acquisition of the seeker.

A. LOWTRAN

The LOWTRAN code calculates both atmospheric transmittance and radiance throughout the infrared spectrum (0.25 to 28.5 micrometers). It uses a single parameter band model for molecular absorption, and includes the effects of continuum absorption, molecular scattering, and aerosol absorption. Refraction and earth curvature are included in the calculation for slant paths.

Five seasonal models and the 1962 U.S. Standard Atmosphere are provided as inputs to the LOWTRAN program using typical altitude, pressure, temperature, water vapor density and ozone density profiles for each. The five other atmospheric profiles consist of (1) Tropical (15° N), (2) Midlatitude Summer (45° N-July), (3) Midlatitude Winter (45° N-January), (4) Subarctic Summer (60° N-July), and (5) Subarctic Winter (60° N-January). With these profiles the user may select the general atmospheric conditions

applicable to the particular simulation. Additionally the user may input radiosonde data if desired to make calculations for a specific profile. Particular information regarding mixing ratios and assumptions made by the LOWTRAN program can be obtained from the LOWTRAN Manual [Ref. 1] and the associated texts listed therein.

The LOWTRAN code includes three boundary layer aerosol types: Rural, Urban, and Maritime. Due to the nature of the SIREM/ASM model, only the latter was used since the composition and distribution of aerosols of oceanic origin are peculiar to the IR/ASM problem. These aerosols are largely sea-salt particles in the lower boundary layer caused by evaporation of sea-spray droplets. Together with a background aerosol of more or less pronounced continental characteristics they form a fairly uniform maritime aerosol which is representative of the lower 2 to 3 kilometers of the atmosphere over the oceans.

These aerosols should not be confused with the heavy direct sea-spray aerosols found in the lower 10 to 20 meters above the ocean surface which is strongly dependent on recent wind velocities and sea surface turbulence. The extinction and absorption coefficients are calculated as a function of the relative humidity and based heavily upon the refractive index for the given altitude and weather conditions.

The ability to calculate slant-path transmittances is incorporated utilizing a data base of seasonal and latitude dependencies of vertical aerosol distributions. This allows transmittance calculations of "high-flyer" missile attack profiles or aircraft infrared missile engagements by changing the input parameters to the LOWTRAN program to match those of the simulation requirements. Iterating this calculation throughout the slant path range values yields the data points necessary to model the reduction in transmittance over the entire engagement-range scenario with a single equation. The horizontal path used by the SIREM model for simulating cruise missiles is assumed to be a constant pressure path where earth curvature and refraction effects are negligible, or taken into account through the use of the 4/3 earth radius model. An alternative flat earth may be assumed for short range situations.

The LOWTRAN code calculates transmittance as a function of "absorber density" for the path, the pressure, and temperature, for the particular wavelength band chosen. It utilizes both empirical laboratory data and available molecular line constant data in performing its calculations. The output for a typical LOWTRAN transmittance run is shown in Figure 4-2. The input to the program for spectral range is in the form of wavenumbers (inverse centimeters). In this example the range is 900 to 1145 cm^{-1} at increments of 5 cm^{-1} required by the LOWTRAN program. The lesser number of

FREQ CM-1	WAVELENGTH MICRONS	TOTAL TRANS	H2O TRANS	CO2+ TRANS	OZONE TRANS	N2 CONT TRANS	H2O CONT TRANS	MOL SCAT TRANS	AEROSOL TRANS	AEROSOL ABS	INTEGRATED ABSORPTION	NITRIC ACID TRANS
900	11.1111	.5943	.9646	1.0000	1.0000	1.0000	.9166	1.0000	.6774	.2614	1.0128	1.0000
905	11.0497	.6183	.9612	.9981	1.0000	1.0000	.9124	1.0000	.6823	.2546	3.0228	1.0000
910	10.9890	.6076	.9600	.9969	1.0000	1.0000	.9140	1.0000	.6808	.2467	5.0105	1.0000
915	10.9290	.6050	.9594	.9960	1.0000	1.0000	.9156	1.0000	.6823	.2399	6.9856	1.0000
920	10.8696	.6090	.9617	.9923	1.0000	1.0000	.9172	1.0000	.6958	.2338	8.9408	1.0000
925	10.8108	.6200	.9775	.9876	1.0000	1.0000	.9187	1.0000	.6953	.2263	10.8465	1.0000
930	10.7527	.6226	.9799	.9823	1.0000	1.0000	.9201	1.0000	.7028	.2195	12.7286	1.0000
935	10.6952	.6236	.9811	.9769	1.0000	1.0000	.9215	1.0000	.7063	.2127	14.6165	1.0000
940	10.6383	.6231	.9783	.9726	1.0000	1.0000	.9228	1.0000	.7097	.2060	16.4352	1.0000
945	10.5820	.6193	.9718	.9693	.9999	1.0000	.9241	1.0000	.7121	.1999	18.3996	1.0000
950	10.5263	.6126	.9657	.9673	.9993	1.0000	.9254	1.0000	.7094	.1976	20.3355	1.0000
955	10.4712	.6096	.9612	.9682	.9985	1.0000	.9266	1.0000	.7068	.1954	22.2939	1.0000
960	10.4167	.6083	.9594	.9676	.9975	1.0000	.9277	1.0000	.7041	.1931	24.2696	1.0000
965	10.3627	.6016	.9587	.9670	.9958	1.0000	.9288	1.0000	.7016	.1919	26.2626	1.0000
970	10.3093	.5962	.9581	.9625	.9931	1.0000	.9299	1.0000	.6998	.1886	28.2659	1.0000
975	10.2564	.5949	.9600	.9625	.9899	1.0000	.9309	1.0000	.6965	.1864	30.3207	1.0000
980	10.2041	.5938	.9663	.9682	.9814	1.0000	.9319	1.0000	.6940	.1842	32.3517	1.0000
985	10.1523	.5966	.9736	.9772	.9719	1.0000	.9328	1.0000	.6916	.1821	34.3669	1.0000
990	10.1010	.6018	.9794	.9862	.9523	1.0000	.9337	1.0000	.6892	.1799	36.4097	1.0000
995	10.0503	.5797	.9782	.9943	.9364	1.0000	.9346	1.0000	.6868	.1777	38.5116	1.0000
1000	10.0000	.5582	.9600	.9971	.9107	1.0000	.9355	1.0000	.6845	.1756	40.7195	1.0000
1005	9.9502	.5379	.9548	.9884	.8867	1.0000	.9363	1.0000	.6796	.1755	43.3345	1.0000
1010	9.9010	.5163	.9472	.9982	.8644	1.0000	.9370	1.0000	.6748	.1754	45.4466	1.0000
1015	9.8522	.4941	.9376	.9964	.8418	1.0000	.9378	1.0000	.6702	.1753	47.9760	1.0000
1020	9.8039	.4837	.9448	.9939	.8246	1.0000	.9385	1.0000	.6656	.1752	50.5577	1.0000
1025	9.7561	.4747	.9433	.9830	.8196	1.0000	.9392	1.0000	.6610	.1752	53.1843	1.0000
1030	9.7087	.4675	.9456	.9845	.8137	1.0000	.9399	1.0000	.6566	.1751	55.9478	1.0000
1035	9.6618	.4362	.9522	.9772	.7643	1.0000	.9405	1.0000	.6522	.1750	58.6650	1.0000
1040	9.6154	.4435	.9565	.9714	.7836	1.0000	.9412	1.0000	.6479	.1749	61.4485	1.0000
1045	9.5694	.4497	.9568	.9625	.8665	1.0000	.9418	1.0000	.6436	.1749	64.0302	1.0000
1050	9.5238	.4782	.9522	.9594	.7959	1.0000	.9423	1.0000	.6394	.1748	66.8393	1.0000
1055	9.4787	.4221	.3480	.9563	.7773	1.0000	.9429	1.0000	.6353	.1747	69.7288	1.0000
1060	9.4340	.4298	.3383	.9557	.8049	1.0000	.9434	1.0000	.6313	.1746	72.5798	1.0000
1065	9.3897	.4450	.3336	.9537	.8441	1.0000	.9439	1.0000	.6273	.1745	75.3545	1.0000
1070	9.3458	.4760	.9393	.9490	.9052	1.0000	.9444	1.0000	.6234	.1745	77.3798	1.0000
1075	9.3023	.5126	.9409	.9482	.9814	1.0000	.9449	1.0000	.6195	.1744	80.4168	1.0000
1080	9.2593	.5525	.9516	.9438	.9899	1.0000	.9453	1.0000	.6157	.1743	82.8041	1.0000
1085	9.2166	.5269	.9518	.9659	.9906	1.0000	.9458	1.0000	.6126	.1742	85.1693	1.0000
1090	9.1743	.5246	.9448	.9753	.9918	1.0000	.9462	1.0000	.6082	.1739	87.5419	1.0000
1095	9.1324	.5229	.9346	.9869	.9918	1.0000	.9466	1.0000	.6043	.1733	89.9277	1.0000
1100	9.0909	.5151	.3192	.9941	.9912	1.0000	.9470	1.0000	.6005	.1728	92.3523	1.0000
1105	9.0498	.5065	.9056	.9983	.9918	1.0000	.9474	1.0000	.5968	.1723	94.8198	1.0000
1110	9.0090	.5013	.9022	.9991	.9906	1.0000	.9477	1.0000	.5931	.1718	97.3101	1.0000
1115	8.9686	.5031	.9101	.9990	.9902	1.0000	.9481	1.0000	.5892	.1715	99.7944	1.0000
1120	8.9286	.5046	.9192	.9990	.9899	1.0000	.9484	1.0000	.5852	.1714	102.2715	1.0000
1125	8.8889	.5057	.9250	.9976	.9896	1.0000	.9487	1.0000	.5813	.1712	104.7432	1.0000
1130	8.8496	.5068	.9374	.9952	.9899	1.0000	.9490	1.0000	.5774	.1711	107.2138	1.0000
1135	8.8106	.4953	.9273	.9911	.9918	1.0000	.9493	1.0000	.5736	.1709	109.7335	1.0000
1140	8.7719	.4970	.9220	.9833	.9928	1.0000	.9496	1.0000	.5698	.1707	112.2983	1.0000
1145	8.7336	.4789	.3181	.9753	.9945	1.0000	.9499	1.0000	.5661	.1706	113.6012	1.0000

INTEGRATED ABSORPTION FROM 900 TO 1145 CM-1 = 113.60AVERAGE TRANSMITTANCE = .5363

2

Figure 4.2. LOWTRAN Program Output

wavenumbers is always the first input into the LOWTRAN program, while the higher wavenumber is the second input. This corresponds to the high-wavelength to low-wavelength output in column 2 of Figure 4-2. The conversion to wavenumbers may be made using the following formulas.

$$\lambda = 10^{-2}/(\text{Wavenumbers}) \quad \text{or}$$
$$\text{Wavenumbers} = 10^{-2}/\lambda \qquad \text{(Eq. 4.1)}$$

Here the wavenumbers are in inverse centimeter values as used by the LOWTRAN program. Transmittance values for each of the contributing absorbers (H_2O, CO_2, Ozone, N_2, Molecular Scattering, Aerosol, and Nitric Acid) are then calculated for each wavenumber (wavelength in column 2) in row format. The total transmittance for each wavenumber is then calculated as the product of the transmittances of each of the absorbing elements and is listed in column 3. The average transmittance listed at the bottom of Figure 4-2 is simply the average of the transmittances in column 3, and reflects the "integrated" overall transmittance across, in this case, the 8.7 to 11.1 micrometer bands for the chosen input parameters (model, visibility, range, etc.).

Since the bandwidth of most IR detectors is limited, either by its own material limitations or external filters, the input wavenumber range will seldom be as wide as the previous example. The 3.5 micrometer band was selected for the development of this paper and consists of wavenumber

inputs of 2850 (lower) to 2860 (upper) cm^{-1}, and correlates to 3.496-3.509 micrometers in 5 cm^{-1} intervals.

In addition to the output shown in Figure 4-2 the program generates a large quantity of "header" information for each run, which reprints the inputs to the program. The unfamiliar user should obtain hardcopy of early runs to see what the output consists of. Once comfortable with the location of various values of the printout, use of the video screen is more appropriate and less wasteful of paper. The objective of each run is the "average transmittance" for the given input parameters, which will later be used in the curve fitting process.

One can easily see that in order to curve fit the transmittance as a function of range with each other parameter held constant, enough runs through the LOWTRAN program must be conducted at "selected ranges" to obtain a smooth curve fit. This means that for every model, range, wind condition, etc. the LOWTRAN program must be run in order to obtain the appropriate transmittance value. This would be a monumental task for the computer, and without stripping the PRINT statements from the LOWTRAN code, could generate a massive output file. The objective here is to show that a minimum number of selected ranges (7 or 8) can be used for this process to decrease computer time spent. The task becomes much easier if a particular set of conditions is in mind, i.e. a Midlatitude Summer model with

average wind conditions of 5 m/s and visibility of 30 kilometers for example. This circumstance could be modelled by running a "stacked input" facility of the LOWTRAN program containing the ranges desired. A test run can be performed to find the approximate maximum range where the transmittance value falls below some operator desired threshold; e.g. T=0.0025.

Curve fitting atmospheric transmittance as a function of range requires that all other parameters (i.e. wind, visibility, etc.) remain constant. Additionally, enough points on the range scale must be taken to provide the necessary accuracy across the span of range of interest. The missile engagement scenario requires that transmittance be a factor in the acquisition process from horizon to target, thus the span in range should be from approximately 20 kilometers to zero. After extensive empirical analysis the values in Table 4.1 were selected to meet the above criteria.

Up to this point it was assumed that all parameters (including wind and visibility) were constant. The desired goal is to analyze the individual effects of wind and visibility on transmittance and develop an empirical equation which generates a good approximation to the transmittance value for any wind and visibility condition over the scenario range, similar to that shown in Figure 4-1. The transmittance takes on a negative exponential

characteristic whose decay constant varies as a function of wind and visibility. The idea is to empirically establish the decay constant as a function of both wind and visibility, the two principal parameters which must remain variable to the model user to realistically model any engagement scenario. Intuitively (and verified by LOWTRAN) atmospheric transmittance decays much more rapidly if either visibility decreases or wind increases. To establish how the decay constant changes with wind and/or visibility, enough values for both wind and visibility must be analyzed to curve fit the decay constant dependence to either. The values of wind and visibility in Table 4.1 were empirically selected and adequately cover the conditions for most scenarios. Then, for each combination of wind and visibility, transmittance values over the range span are obtained using LOWTRAN. This builds a 3-dimensional table which is tha basis for curve fitting and establishing the decay constant as a function of three variables; i.e. range, visibility, and wind.

TABLE 4.1. RECOMMENDED CURVE FIT DATA POINTS

Range in Km	Wind m/s	Visibility in Km
0.2	0.1	40
1.0	5.0	30
2.0	10.0	20
4.0	15.0	15
8.0	20.0	10
12.0		
18.0		
21.0		

The method used for data reduction is an extremely simple technique implemented for microcomputer spreadsheets. The method employs a scheme for performing Weighted Least Squares curve fit techniques to the data, and while calculating the coefficients of the curve fit, the goodness of fit of the curve to the data may be viewed graphically by the modeller for approval or correction as necessary. Some examples of the process will be given later.

The LOWTRAN program serves as an excellent tool for calculating transmittance over a wide variety of parameters, however, the program consists of 9000 lines of FORTRAN code. Most simulations are already quite large, and the addition of this code size as a subroutine is undesireable, considering that each increment in range of the missile flight path must vector to LOWTRAN as a subroutine in order to obtain an updated single transmittance value.

The alternative method presented here for obtaining the transmittance value desired is by utilizing LOWTRAN external to the simulation and curve fitting the output data points as a function of range to a single equation, given the visibility and wind conditions of the particular engagement. This method requires extensive use of the LOWTRAN program to obtain the data points necessary to perform the curve fit. Once completed though, the two coefficients of the

approximated curve are the only data necessary to write an equation of the form:

$$T = \sigma \, Exp(-\alpha R) \qquad \text{(Eq. 4.2)}$$

The coefficients of this equation (σ and α) are all that is necessary to allow calculation of transmittance as the missile moves incrementally through the stochastic simulation. When an increment inrange occurs, a vector to the transmittance calculating subroutine (or function) with this equation updates the transmittance affect on the probability of acquisition. As previously discussed, the decay constant (α) is actually a function of wind and visibility. Later in this chapter accomodations will be made for this.

The SIREM model specifically calculates through simulation, the effectiveness of deployment of Torch/PIP Torch type infrared decoys against infrared seeking anti-ship missiles (ASMs). It is assumed from this point on that the incoming missiles utilize a "low altitude" attack profile typical of the cruise missile variety which prevents early detection by the target ship. Assume for the time being that it flies at an altitude of approximately 60 feet (20 meters from the LOWTRAN example modelled herein). This would constitute a horizontal transmittance path when using the LOWTRAN program to calculate transmittance throughout the missile-to-target flight path. Some other assumptions

utilized in the empirical derivations in this paper which were used as inputs to the LOWTRAN program are:

a) The Marine Atmospheric Boundary Layer model was the only one utilized.

b) A land haze factor of 3 was used (default).

c) The wavelength modelled here was 3.5 micrometers.

d) Each of the 6 atmospheric profiles was calculated.

e) Default parameters inherent to LOWTRAN were used, varying only the visibility conditions, range, and wind conditions

f) There was no precipitation.

Each of these parameters may be changed if desired to meet an alternative modelling requirement. For example, if it is known that a "new" IR missile threat has evolved which utilizes a "high-flyer" attack profile and a 3.2 micrometer optimized detector, the modeller could then choose the slant-path option in the LOWTRAN program selected at the necessary wavelength. Knowing only the flight profile, detector frequency(ies) and atmospheric conditions would then allow full use of the empirical transmittance modelling technique presented here without insertion of 9000 lines of LOWTRAN code.

Another advantage to this approach other than its simplicity and accuracy is that, if the simulation is written in a language other than FORTRAN, this method can still be easily adapted due to the short code length

required using the standard exponential function. The equational form is easily translated as will be seen.

Let's analyze an example scenario. Suppose we are faced with our ship-versus-missile engagement described previously, and wish to calculate atmospheric transmittance at various ranges in order to approximate its affect on the acquisition process. First we must assume some meteorological conditions appropriate to our example for inputs to the LOWTRAN program. We will select here the parameters:

1) Midlatitude Summer profile.
2) Visibility is 30 kilometers.
3) A maritime environment.
4) A land haze factor of 3 (may vary from 1 to 10, with 10 being bad haze as around Los Angeles).
5) Wind is virtually nill. (0.1 m/s) and has been so for the past 24 hours.
6) The range from the seeker to target is 4 kilometers.
7) Assume a 3.5 micrometer band (2850-2860 cm^{-1})
8) The path is horizontal at 20 meters altitude.

We may now insert out data into the LOWTRAN program in the format listed in the LOWTRAN Manual [Ref. 1].

In doing so we would find that at our 4 kilometer range, the transmittance for this wavelength would be 0.6516 (See Appendix A: Table A.2.a). The value may differ only slightly between computers. This means that the received

energy density at a range of 4 kilometers is only 65% as high as that for a perfectly transmitting medium (vacuum). We can now duplicate our efforts for the 4 kilometer range, but now with a wind velocity of 10 meters per second, keeping visibility the same. Doing this we obtain a transmittance value of 0.4537. In the diagram below we see that increasing the wind, or decreasing visibility, has a dramatic effect on the decay constant associated with the transmittance.

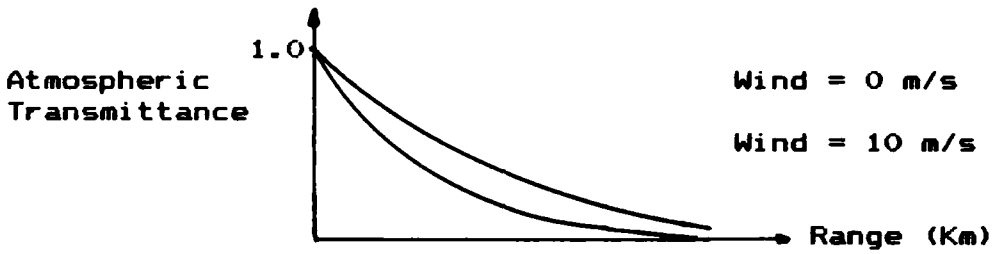

Figure 4-2. Wind Effects on Transmittance.

Note the approximately exponential fall off with range. This is the curve we wish to approximate as:

$$T(R,V,W) = \sigma \cdot EXP(\alpha(V) \cdot f(W) \cdot R \cdot \delta) \qquad \text{(Eq. 4.3)}$$

from the data points obtained from the LOWTRAN program. Here T, R, V, and W represent transmittance, range, visibility, and wind respectively. There is correlation between wind and visibility, and the effects are accounted for in the factor δ.

In order to model any particular atmospheric profiles, the data points for the 3-dimensional table may be obtained by adapting the following overlay algorithm as the main program, using LOWTRAN as a subroutine.

```
FOR Atmospheric_Profile - 1 to 6          * See Note 1
  FOR Wind_Speed = 0 to 20 Step 5         * See Note 2
   Wind = 0.01 + FLOAT(Wind_Speed)
    FOR I = 1 to Nr_of_Range_Values
     READ Range_Value
     OPEN Input_File                      * See Note 3
     WRITE Input_File
     CALL LOWTRAN
     WRITE Output
    NEXT I
   NEXT Visibility
  NEXT Wind_Speed
 NEXT Atmospheric_Profile
```

Note 1: Prior to entering the looping structure the user must assign values to the other parameters used by the LOWTRAN program (e.g. wavenumbers, haze factor, etc.).

Note 2: The actual wind speed may not be zero. If so LOWTRAN defaults to 4.1 m/s. Hence the following statement.

Note 3: The input file must be formatted as specified in the LOWTRAN Manual [Ref. 11].

Again it should be emphasized that the source code of the LOWTRAN program should be commented out to prevent printing of the massive administrative data. Only the "Average Transmittance" over the sufficiently narrow band is desired. The output may be directed to a printer or file. The latter method is preferred if input to the curve fitting process is desired in a direct fashion. In order to keep track of which data value is associated with which range, visibility, and wind value, it may be wise to write those associated values in the same output row.

Continuing with our example we will assume for now that only one value for wind, and likewise visibility are calculated. The transmittance would then become only a function of range since all other parameters remain constant. The desired goal is to select range values which best facilitate the curve-fitting process. Using the range values from Table 4.1 we can now perform an example of the curve fitting process, while presenting the spreadsheet technique used for doing Weighted Least Squares.

1. Example

Making the assumption that all parameters remain constant as before, with only range changing, a curve fit of the following LOWTRAN data is performed for the Midlatitude Summer profile with wind at 5 meters per second, and visibility of 30 kilometers.

TABLE 4.2a. LOWTRAN DATA FOR CURVE FITTING

RANGE	TRANSMITTANCE	WEIGHTING FACTOR
0.2	0.9272	8
1.0	0.7824	1
2.0	0.6588	2
4.0	0.4828	21
8.0	0.2723	6
12.0	0.1588	1
18.0	0.0727	1
21.0	0.0498	2

The Weighted Least Squares procedure is conducted in two parts. To effect the weighting, implementing multiple occurrence of the same data points is shown in table 4.3. Following in figure 4.4a and 4.4b is the actual Least Squares algorithm implemented in spreadsheet format. The output desired is the values for the A-Coefficient (σ) and B-Coefficient (α) for equation 4.2. In this example the first coefficient σ=0.875824, and the second, α=-0.140899. Using equation 4.2 yields the table which follows at the top of the following page.

TABLE 4.2b. DATA POINTS EXTRACTED FROM FITTED CURVE

RANGE	TRANSMITTANCE
0.2	0.8515
1.0	0.7607
2.0	0.6607
4.0	0.4985
8.0	0.2837
12.0	0.1615
18.0	0.0693
21.0	0.0454

Comparing table 4.2a with 4.2b (i.e. the LOWTRAN data versus the exponential Curve-Fitted data) we notice comparable transmittance values, especially at ranges greater than one kilometer. Due to the nature of the engagement scenario, we may assume transmittance values at ranges less than one kilometer or so to be equal to 1.0, since its effect on acquisition at these ranges is minimal. Above 1 kilometer the error is generally one to two percent at most, and hence, very useable for "probability" modelling. Within the following tables the Least Squares process in implemented into spreadsheet format. Although in this case Lotus Development Corporation's 1-2-3 (TM) was used, the technique is similar if using commercially available packages. The data is arranged in row-versus-column format with the Least Squares algorithm implemented in Tables 4.4a and 4.4b.

	A	B
1:	Model:	Midlat Sum
2:	Visibility:	30
3:	Varied param:	Visibility
4:		
5:	Range (km)	Transmittance
6:	0.2	0.9272
7:	0.2	0.9272
8:	0.2	0.9272
9:	0.2	0.9272
10:	0.2	0.9272
11:	0.2	0.9272
12:	0.2	0.9272
13:	0.2	0.9272
14:	1	0.7824
15:	2	0.6588
16:	2	0.6588
17:	4	0.4828
18:	4	0.4828
19:	4	0.4828
20:	4	0.4828
21:	4	0.4828
22:	4	0.4828
23:	4	0.4828
24:	4	0.4828
25:	4	0.4828
26:	4	0.4828
27:	4	0.4828
28:	4	0.4828
29:	4	0.4828
30:	4	0.4828
31:	4	0.4828
32:	4	0.4828
33:	4	0.4828
34:	4	0.4828
35:	4	0.4828
36:	4	0.4828
37:	4	0.4828
38:	8	0.2723
39:	8	0.2723
40:	8	0.2723
41:	8	0.2723
42:	8	0.2723
43:	8	0.2723
44:	12	0.1588
45:	18	0.0727
46:	21	0.0498
47:	21	0.0498

TABLE 4.3.

TRANSMITTANCE AND RANGE DATA POINTS USED

NOTE:

Using the same data point multiple times at any point minimizes error about that point in the curve fit process. This emulates the weighting matrix commonly used in performing Wieghted Least Squares curve fitting.

TABLE 4.4a. CALCULATIONS USED IN LEAST SQUARED FITTING

	C	D	E	F
1:	SUM of R_i	This section finds the coefficients		
2:		A and B for the equation:		
3:	210.6	$T = \delta * Exp(\alpha * R)$.....at Visibility =30 km		
5:	R_i^2	$Ln(T_i)$	$[Ln(T_i)]^2$	$R_i * Ln(T_i)$
6:	0.04	-0.0756	0.0057	-0.0151
7:	0.04	-0.0756	0.0057	-0.0151
8:	0.04	-0.0756	0.0057	-0.0151
9:	0.04	-0.0756	0.0057	-0.0151
10:	0.04	-0.0756	0.0057	-0.0151
11:	0.04	-0.0756	0.0057	-0.0151
12:	0.04	-0.0756	0.0057	-0.0151
13:	0.04	-0.0756	0.0057	-0.0151
14:	1	-0.2454	0.0602	-0.2454
15:	4	-0.4173	0.1742	-0.8347
16:	4	-0.4173	0.1742	-0.8347
17:	16	-0.7282	0.5302	-2.9126
18:	16	-0.7282	0.5302	-2.9126
19:	16	-0.7282	0.5302	-2.9126
20:	16	-0.7282	0.5302	-2.9126
21:	16	-0.7282	0.5302	-2.9126
22:	16	-0.7282	0.5302	-2.9126
23:	16	-0.7282	0.5302	-2.9126
24:	16	-0.7282	0.5302	-2.9126
25:	16	-0.7282	0.5302	-2.9126
26:	16	-0.7282	0.5302	-2.9126
27:	16	-0.7282	0.5302	-2.9126
28:	16	-0.7282	0.5302	-2.9126
29:	16	-0.7282	0.5302	-2.9126
30:	16	-0.7282	0.5302	-2.9126
31:	16	-0.7282	0.5302	-2.9126
32:	16	-0.7282	0.5302	-2.9126
33:	16	-0.7282	0.5302	-2.9126
34:	16	-0.7282	0.5302	-2.9126
35:	16	-0.7282	0.5302	-2.9126
36:	16	-0.7282	0.5302	-2.9126
37:	16	-0.7282	0.5302	-2.9126
38:	64	-1.3009	1.6922	-10.4068
39:	64	-1.3009	1.6922	-10.4068
40:	64	-1.3009	1.6922	-10.4068
41:	64	-1.3009	1.6922	-10.4068
42:	64	-1.3009	1.6922	-10.4068
43:	64	-1.3009	1.6922	-10.4068
44:	144	-1.8401	3.3860	-22.0813
45:	324	-2.6214	6.8718	-47.1855
46:	441	-2.9997	8.9984	-62.9945
47:	441	-2.9997	8.9984	-62.9945
48:	$Sum(R_i)^2$	Sum $Ln(T_i)$	Sum Squares	Sum of Products
49:	2079.3200	-35.2421	49.9966	-320.8972

TABLE 4.4b. SPREADSHEET LEAST SQUARES CALCULATIONS

	G	H		Formula in cell at left: Note: Here n=42
1:	Scratchpad		:	
2:	-0.1409		>	(42*F49-D49*C3)/(42*C49-C3^2)
3:	-0.1326		>	(D49-G2*C3)/42
4:	20.3153		>	G2*(F49-C3*D49/42)
5:	20.4251		>	E49-D49^2/42
6:			:	
7:	A-Coefficient	0.875824	>	Exp(G3)
8:	B-Coefficient	-0.140899	>	G2
9:	R-Squared	0.9946	>	G4/G5

This satisfies the Least Squares process. Cells G2 through G5 represent respectively:

G1) $[n\Sigma(R_i \ln(T_i)) - \Sigma \ln(T_i)\Sigma R_i]/[n\Sigma R_i^2 - (\Sigma R_i)^2]$

G2) $[\Sigma \ln(T_i) - (G1)(\Sigma R_i)^2]/n$

G3) $G2\ [\Sigma R_i \ln(T_i) - \Sigma R_i \Sigma \ln(T_i)/n]$

(Eq. 4.4-4.7)

G4) $\Sigma \ln(T_i)^2 - (\Sigma \ln(T_i))^2/n$

Cell C3 is the sum of the range values of column "A".

C3) ΣR_i (Eq. 4.8)

The R-Squared value represents the "Goodness of Fit" of the function to the original data when using the approximating equation. In this case the fit is a very one, but in cases of either extremely good or poor visibility (i.e. >40 or <5 kilometers) errors between LOWTRAN predictions and empirical results grow, and the fitted curve will have regions where error may be on the order of five to six percent. For modelling in the probabilistic sense this

is still adequate, since the region of error is transient and errors of this magnitude have only small effects on the acquisition probability. Figure 4-3 is a plot of the above example using both LOWTRAN-obtained data points, and the corresponding exponential curve fit data points obtained by using the spreadsheet technique presented. We may now extend our process to calculate the atmospheric transmittance for any of the 6 LOWTRAN profiles for any wind or visibility conditions.

Figure 4-3

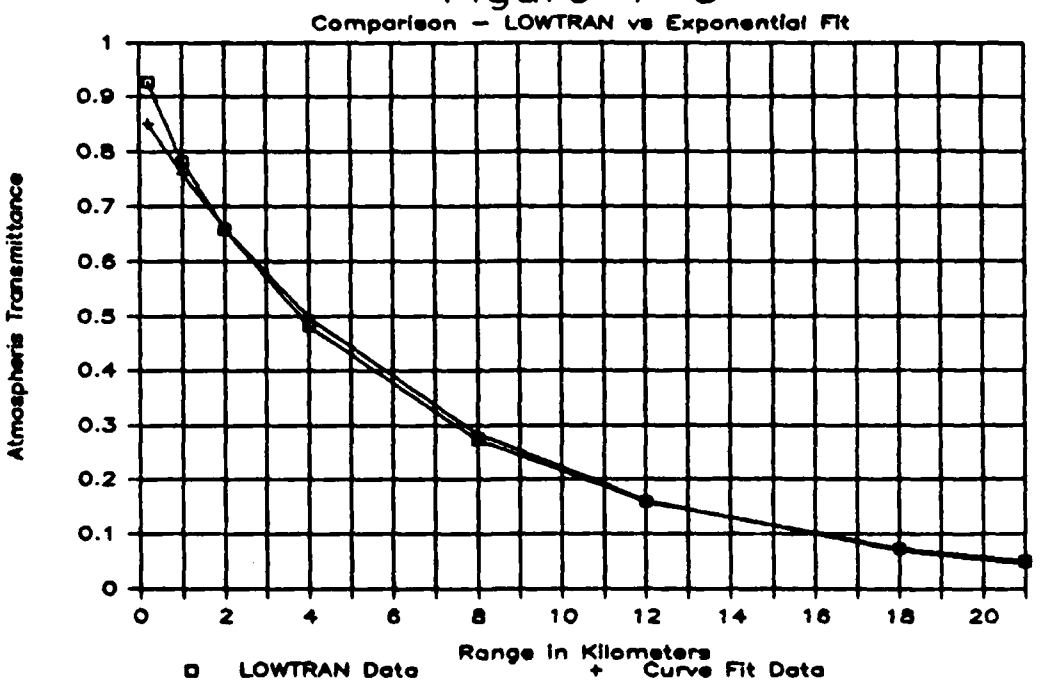

a. Extending the Curve Fit

The 3-dimensional table (A.2.a) of transmittance values has been obtained for, in this case, the Midlatitude Summer Profile. Thus far we have completed the curve-fitting process for one particular wind and visibility condition (i.e. visibility of 30 Km, wind speed 5 m/s as calculated in Table 4.4). The A and B coefficients (σ and α), which were derived as a result of Least-Squares fitting an exponential function, were used in equation 4.2 to emulate extinction over range for <u>this</u> wind/visibility combination to obtain Figure 4-3. There the accuracy of the exponential fit versus the original LOWTRAN data is visually apparent. Tables A.1.a through A.6.b in Appendix A list the values of transmittance obtained from the LOWTRAN program <u>and</u> from the curve fitting process for each of the six atmospheric profiles available. The curve-fit coefficients for the other five atmospheric profiles are contained in Tables A.7 and A.8 in Appendix A.

We now wish to extend this procedure to be able to emulate extinction over range for <u>any</u> wind/visibility combination. To do so we must first build a table of the A and B coefficients and examine how their values change from one wind/visibility combination to another. Using the combinations from Table 4.1 the coefficients were obtained

for the entire atmospheric profile of our example. These are contained in Table 4.5.

By examining Table 4.5 we see that the A coefficients hardly change throughout entire range of wind and visibility values. This coefficient may be assigned a constant value for the remainder of the extinction curve-fit process. This is true when modelling each of the atmospheric profiles individually; however, the A-coefficient does change from one profile to another. This can be seen in Table A.7 in Appendix A.

TABLE 4.5. EXPONENTIAL CURVE FIT COEFFICIENTS FOR "MIDLATITUDE SUMMER" PROFILE

A-Coefficient Value

Wind	Vis=40	Vis=30	Vis=20	Vis=15	Vis=10
0	0.875788	0.875808	0.875754	0.875834	0.875812
5	0.875747	0.875824	0.875699	0.875477	0.877011
10	0.875820	0.875716	0.875650	0.874656	0.874052
15	0.875753	0.875685	0.875366	0.876011	0.872420
20	0.875777	0.875885	0.875886	0.877431	0.859462

B-Coefficient Value

Wind	Vis=40	Vis=30	Vis=20	Vis=15	Vis=10
0	-0.064275	-0.065945	-0.069313	-0.072711	-0.079494
5	-0.118579	-0.140899	-0.185840	-0.231112	-0.322254
10	-0.129858	-0.156395	-0.209959	-0.263693	-0.371488
15	-0.132919	-0.160663	-0.216479	-0.273163	-0.384626
20	-0.134394	-0.162714	-0.219772	-0.277832	-0.386820

The B-coefficients do vary throughout Table 4.5. Through further examination, the change in its value is non-linear with wind and visibility, and as such, simple linear

interpolation of this table is not accurate. Nor is this technique desirable because it requires many more B-coefficient data points than those contained in Table 4.5 to be stored in memory to be even moderately accurate. The process of extending equation 4.2 to the more general form of equation 4.3 becomes a matter of finding out how the B-coefficients in Table 4.5 change as a function of wind and visibility (i.e. find the exponential decay constant of extinction in terms of its dependence on wind and visibility), and fit functions which will accomodate the 2-dimensional decay constant variation.

Thus the curve fit process is continued, only now it must be performed on the B-coefficients which vary with both wind and visibility. This will leave 'Range' as the only variable to input to equation 4.3 for calculating transmittance. From table 4.5 it can be seen that the B-coefficient increases negatively (decreases) as either 1) wind increases, or 2) visibility decreases, and is therefore a function of wind and visibility. Equation 4.3 stipulates that the decay constant for extinction over range consists of three parts. These are:

a) $\alpha(V)$ - Due to changes in visibility,

b) $f(W)$ - Due to changes in wind, and

c) δ - Any correlation between the first two.

By also observing that the B-coefficient is least negative where wind is minimum and visibility is maximum, we can now use the ratios of any other B-coefficients relative to the first and find their multiplicative increase over the original (baseline - maximum visibility, minimum wind) B-coefficient due to wind and visibility. This done by dividing each value in the B-coefficient table by the 'baseline' value in the upper left corner of the table as is done for Table 4.6. Table 4.6 depicts how much greater (negatively) the decay constant is for any particular wind and visibility combination than it would be for its best transmittance (i.e. wind zero, visibility maximum). The non-linearity of the B-coefficient with wind or visibility is much more evident in Table 4.6. We shall see in a few moments why this table is necessary.

TABLE 4.6. RATIO OF B(Vis,Wind) TO B(Vis_{MAX},$Wind_{MIN}$)

Wind	Vis 40	Vis 30	Vis 20	Vis 15	Vis 10
0	1.0	1.02598	1.07838	1.13125	1.23678
5	1.84487	2.19213	2.89133	3.59567	5.01367
10	2.02035	2.43322	3.26657	4.10257	5.77966
15	2.06797	2.49962	3.36801	4.24991	5.98407
20	2.09092	2.53153	3.41924	4.32255	6.01820

The following steps are the procedures used to obtain the three functions of the exponential decay constant of equation 4.3. Individually these steps produce the functions $\alpha(V)$, $f(W)$, and δ which will allow the input of

any wind or visibility value from 0-20 m/s or 40-5 km respectively, and generate the approximated B-coefficient of extinction for that condition. Keep in mind that this example only covers the 'Midlatitude Summer' profile. The other profiles are approximated in the same fashion, with the results included in Table 4.7.

(1) Step One. As visibility decreases the B-coefficient becomes more negative, causing transmittance to decrease at a faster rate (more extinction). Testing of various functions was conducted to generate the B-coefficient as a function of visibility. It was assumed to start with that wind is zero so that the curve fit process uses the B-coefficients of the first row on Table 4.5. Graphically the data points appear as in Figure 4-4.

Figure 4—4

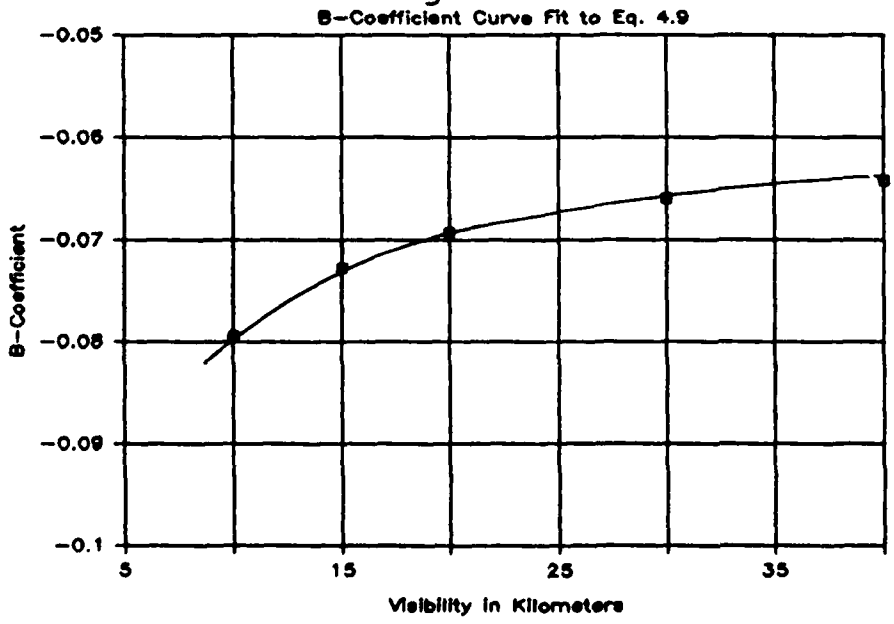

Care must be taken in selecting a curve-fit method to approximate any of the three functions $\alpha(V)$, $f(W)$, or δ since the B-coefficient data points are negative. This eliminates exponential or logarithmic function Least-Squares techniques since the natural logarithms of the data points are necessary, and are undefined.

To approximate $\alpha(V)$, a cubic function was selected of the form:

Row [α(Vis)]: $A_1 + A_2 \cdot V + A_3 \cdot V^2 + A_4 \cdot V^3$ (Eq. 4.9).

This eliminated the negative data point problem and produced highly accurate results for the few data points on hand. The values found for the coefficients of the cubic are contained in Table 4.7. These values were used to generate the fitted curve in Figure 4-4, while the original B-coefficients were plotted as the single point values. Remember: fitting of this function is performed only on the first row of B-coefficients in Table 4.5.

(2) Step Two is to establish a function which reflects the change in the decay constant with wind: i.e. $f(W)$. Graphically the data points plot as shown in Figure 4-5. At first the function appears as an exponential decay which would be easily modelled. But, since the data points are negative this method is not easily performed. This is where the concept of Table 4.6 is useful. Given that the B-

Figure 4—5

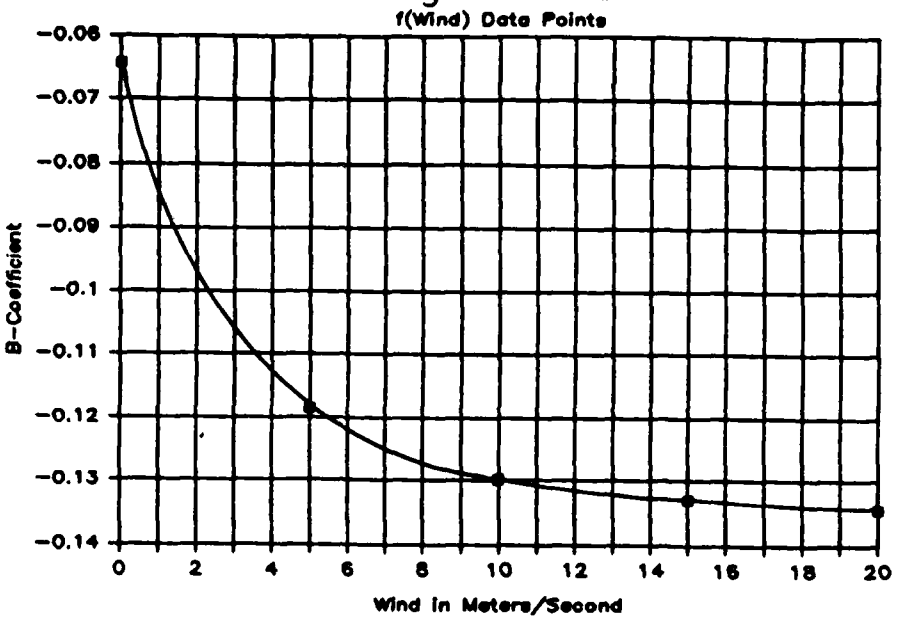

Actual B-coefficient change with increasing wind.

Figure 4—6

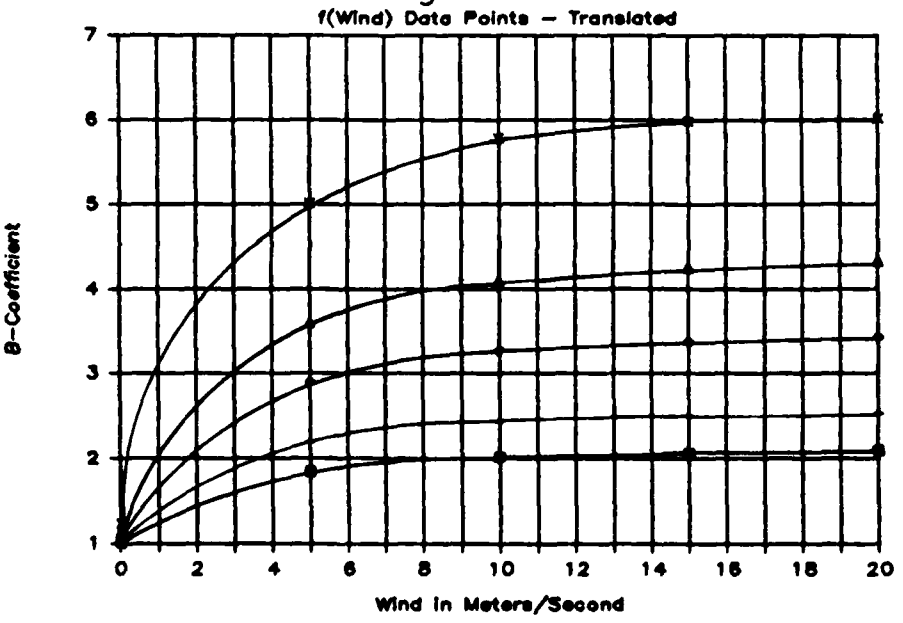

B-coefficient translated for curve-fit to Eq. 4.]0.

coefficient for any visibility condition (with wind zero) can be generated by completing step one, then f(W) becomes merely a multiplier to that value generated.

To find out what to multiply $\alpha(V)$ by to get the decay constant for wind conditions which are not zero, we fit a function to the first column of Table 4.6. Now, all the data points are positive, and any function is fair game. Graphically, the newly translated function appears as in Figure 4-6. After unsuccessful (inaccurate) attempts to fit a hyperbolic tangent (tanh) function to this curve, a much more accurate one was discovered:

$$\text{Column [f(Wind)]:} \qquad 1+[D_1 \cdot (1-\text{Exp}(D_2 \cdot \text{Wind}))] \qquad \text{(Eq. 4.10)}$$

(3) Step Three. Figure 4-6 shows a family of five curves which plot each of the five columns of Table 4.6. The curve with the least maximum represents the first column in Table 4.6. The others in increasing fashion represent decreasing visibility conditions. The correlation factor δ is necessary to increase the extinction when wind and visibility are not zero and maximum respectively. In this case δ acts as a multiplier also, driving the decay constant more negative when its value becomes greater than one. Fitting a function to points vertically spaced on Figure 4-6 is the key to finding the correlation coefficient δ. A function which works extremely well in this case is:

$$\delta = C_1 \cdot V^{C_2} \qquad \text{(Eq. 4.11)}$$

The same effect may be obtained by fitting equation 4.11 to the data points of one of the lower rows of Table 4.6 if they have been normalized a second time in the horizontal direction (i.e. divide each coefficient in one lower row of Table 4.6 by the coefficient in the first column of that row).

This procedure completes the curve fitting process for each atmospheric profile, leaving eight constant coefficients which, when incorporated into equation 4.3, yield an admirable approximation of transmittance values at range values between one and twenty kilometers throughout the entire atmospheric profile. This procedure was used to establish the constants for each of the six LOWTRAN profiles. These constants are included here for reference.

TABLE 4.7

CURVE FIT COEFFICIENTS FOR ALL SIX LOWTRAN PROFILES

	TROPICAL PROFILE	MIDLATITUDE SUMMER	MIDLATITUDE WINTER
A_1	-0.139154	-0.1249852	-0.08956
A_2	6.2887E-03	6.296102E-03	6.317317E-03
A_3	-2.2354E-04	-2.207060E-04	-2.247950E-04
A_4	2.6091E-06	2.619482E-06	2.627775E-06
C_1	13.74105	15.18516	29.876
C_2	-0.716806	-0.743405	-0.923857
D_1	0.895	1.10	2.46
D_2	-0.30	-0.27	-0.295
σ	0.880	0.875	0.9383

TABLE 4.7 (Continued)

	SUBARCTIC SUMMER	SUBARCTIC WINTER	STANDARD ATMOSPHERE
A_1	-0.109255	-0.07970	-0.091037
A_2	6.2545E-03	6.4225E-03	5.6255E-03
A_3	-2.2228E-04	-2.2857E-04	-2.0021E-04
A_4	2.5953E-06	2.6723E-06	2.3407E-06
C_1	19.1121	37.730	24.130
C_2	-0.80492	-0.98561	-0.86706
D_1	1.440	3.980	1.812
D_2	-0.30	-0.2825	-0.34
σ	0.	0.9636	0.9208

Note here that eight of the nine constants in each atmospheric profile eventually constitute α, the 'B' or extinction coefficient. The next step is to implement and explain the computer coding process. This procedure is contained in appendix B. We can now turn our attention to the SIREM model and examine the acquisition process.

V. THE STOCHASTIC INFRARED ENGAGEMENT MODEL (SIREM)

As discussed in chapter one, the most inexpensive means of developing equipment characteristics and tactics for their use is through simulation. The use of computers to analyze effectiveness of systems or subsystems is becoming the predominant development method for this reason. The SIREM model was designed to investigate the effectiveness of deploying decoys which emit an infrared signature against infrared seeking anti-ship missiles (ASMs).

By examining through simulation such parameters as burn time, deployment altitude, deployment angle, decoy drift and descent characteristics if airborne, and distance from the ship, optimum design requirements and deployment tactics can be developed. As with any software model, to maintain its validity it must be periodically reviewed and upgraded to remove any synthetic qualities and replace them with accurate representations.

There are ongoing efforts to incorporate atmospheric losses, discriminative seeker capabilities, and last but not least the multi-ship multi-missile analysis capability. Coincident with the work being done on the SIREM model, extensive investigation is being conducted regarding optimum deployment characteristics for chaff, repeater decoys, and a

variety of other offboard countermeasures in order to integrate the use of offboard devices into a multi-band defensive system. To fully understand the SIREM model requires extensive programming experience and/or simulation expertise. Likewise an operational knowledge of available devices is advisable; however, a general description of the program is in order.

A. THE MODEL

The SIREM model calculates probabilities associated with distraction of an IR homing missile by a pattern of decoys launched by the attacked ship. Rather then the Monte Carlo method of simulation, a stochastic approach was utilized in order to significantly reduce computation time. The program uses realistic input parameters pertinent to the scenario under study, and evaluates statistical information about the distraction effectiveness which may be output in graphical or numeric form.

The user may easily modify any of the input parameters under the following general headings:

1. Ship characteristics
2. Missile characteristics
3. Decoy characteristics
4. Scenario and run characteristics

Although the original version transported from Naval Research Laboratory was designed to operate under the NLX NAMELIST facility of the Prime (TM) computer there, significant changes were required to adapt the input/output to non-NAMELIST type since it was not available at Naval Postgraduate School; and to modify the graphics subroutines and hardware to operate on the Digital VAX 11/780 (TM) and the DI-3000 (TM) graphics software available there.

Output from the program is available in the form of graphs or printed output. A summary of the available graphs is listed here:

1. Probability of distraction conditioned on initial missile-to-ship distance.
2. Probability of distraction conditioned on initial azimuthal approach angle.
3. Pattern of ship lock-on range as a function of angle.
4. Probability of distraction conditioned on initial azimuthal approach angle and a single initial missile to ship distance.
5. Angular regions where probability of distraction exceeds a threshold.
6. Locations where threshold crossings of plot 5 occur.
7. Probability of distraction conditioned on initial missile-to-ship distance and sector of initial azimuthal approach angle.
8. Ship orientation, decoy deployment, and wind direction.
9. Effects of atmospheric refraction on IR at various incidence angles.

Being stochastic by design, certain parameters may be considered random variables for initialization. The initial position and orientation of the missile relative to the ship is a good case. It is assumed for startup that the missile is pointed radially inward toward the ship, and hence the effectiveness computations would yield a lower bound for effectiveness of decoy distraction. This is the basis for the 'worst case' situation described in earlier chapters.

The initial range and azimuth approach angle of the missile are discrete random variables. The initial range may be changed to appropriate kilometer values; while the initial range may also be modified, it is designed to run multiple missiles at the ship every $360/N_{THETA}$ degrees.

The seeker characteristics and the random variables assigned to emulate it can change from missile to missile. In this sense, randomness must be assigned to accomodate scanning directions, boresight error, field of view, and probability of acquisition on multiple targets (i.e. ship plus any decoys). The model performs these adequately, using significant but valid assumptions regarding the process.

The maximum initial range of the missile to the target is R_o at the time of launch of the first decoy. This is considered time t=0. It then takes R_o/V_M seconds for the missile to reach the ship at the origin, with V_M being the missile velocity. The sample time T_s interval determines

the maximum number of time samples taken N_{Ts}. T_t is set small enough to obtain an accurate representation of the scenario. Since the missile is always aimed at ship before acquisition, a lower bound on distraction results, and if no decoy is acquired then the probability of distraction is zero for that given initial range and azimuth.

The choice of time interval T_t is dependent on the missile velocity, target velocity, and the scanner sweep time T_s. Since the area of the scanner field of view on the sea surface is large relative to the distance either the missile or ship travels during the sweep time, T_s may equal T_t. As different conditions arise a necessity for time scaling may result. Developments have begun to incorporate different scanner parameters.

The projection of field of view is incorporated to allow both curved earth and flat earth calculation. The ship and decoys are treated as point targets for infrared radiator purposes. The "hot spot" of the deployed decoy is placed at a known distance above the sea surface. Calculations are made to determine if the hot spot is within the field of view of the scanner. The next stage of development requires incorporating radiance and transmittance calculation, and detector sensitivity parameters to determine if there is sufficient radiance from the ship or decoy to be detected by the seeker. Much of this development was covered in earlier chapters.

The model can also calculate any shadowing of decoys by the ship. This means that if the aspect of the ship comes between the missile and decoy, effectiveness of that decoy will inherently drop to zero. This can be done using either the flat or 4/3 earth model. In addition to shadowing by the ship, if excessive range exists, shadowing by the earth may occur.

Once acquisition of a decoy occurs, the missile flies according to the aerodynamic parameters of the control surfaces and systems for whatever missile is being modelled. If a decoy is not in the field of view and the ship is acquired, the missile is assumed to hit the ship. If locked onto a decoy, the missile flies at the decoy until it passes it. At that point break-lock occurs. This condition may also occur if the control system forces the missile to maneuver so that the decoy is no longer in the field of view. And lastly, if the decoy burns out break-lock occurs.

When break-lock occurs the scanner must re-enter the acquisition mode. Since the missile usually makes drastic maneuvers near break-lock, the re-acquisition process is somewhat random, but if the ship is in the field of view it may be assumed to hit the ship. Missile flight continues at break-lock until all targets are passed.

The flexibility of the program is excellent. Virtually any parameter is changeable either at input or at source code level. As many as five decoys may be deployed by the

ship (more if certain array dimensions are changed) in any combination of deployment angles, times, altitudes, and active lifetime. The ship may change size and speed. The wind is a factor on decoy drift and missile flight. And the missile may change speed, altitude of approach, and control system or seeker parameters. The variations are endless, and analysis of the many combinations pertinent to real-world scenarios may be undertaken to make maximum effective use of offboard countermeasures. Additionally, by further extending not only SIREM but other similar models as well, evaluation of descrimination techniques and optimization of decoy signatures become possible avenues of further development. With this in mind we turn our attention to the acquisition process and observed phenomena.

VI. IR SEEKER SYSTEM AND COUNTERMEASURES

Since the principal interest here lies in passive seekers, it is convenient to separate these into three broad categories: (1) Scanning systems such as search, track, and imagers, (2) Staring systems which use non-mechanical means to obtain spatial scene viewing, and (3) Measurement systems such as radiometers, spectrometers and interferometers. Of interest here are the first two categories. Scanning detection schemes are most common since staring systems usually require sophisticated multi-dimensional array detectors and massive numbers of amplifiers to support the individual elements.

A. SCANNING AND STARING SYSTEMS

Scanning systems sample the radiant intensity distribution in their field of view using various horizontal/vertical techniques. The output from the detector in this case will be a linear analog of the distribution or a simple indication of the presence of a target and its location. The object plane is usually assumed at infinity and the detector responds to radiant levels within the instantaneous field of view of its element(s). This gradient in radiance is translated to

electrical signals which are then filtered, amplified, and referenced to a baseline (missile axis) for inputs to the various azimuth and elevation control systems. For imaging systems the signal is translated from the object to its corresponding image plane by painting out the radiance distribution using optical deflection onto a film, or beam deflection to a cathode ray tube. Using internal processing techniques in missile seekers, the translation is used as input to the missile control surface system to center the highest radiant intensity in the center of the total field of view. The use of either spiral or raster techniques to accomplish slow mechanical scanning is most common. In some cases the relatively high speed motion at altitude provides the vertical trace capability for the system, while a spinning mirror provides the horizontal trace. Regardless of the scanning technique employed, major concern has recently been given to the incorporation of discrimination processing into newer seeker systems. If (or, more appropriately, <u>when</u>) this occurs, the effectiveness of using offboard decoys could be significantly reduced. Therefore, an examination of possible discrimination methods is in order.

In dealing with imaging systems there are two basic approaches to describe the sensitivity of the detector. The first approach is based on the detector figure of merit (D^*) described earlier. It regards the detector as a noise

source of fixed level which is determined from the measurements of fixed conditions similar to those encountered by the detector when installed in its normal operating configuration inside the seeker.

The other approach which is suitable only for BLIP (Background limited mode) detectors regards a random arrival rate of photons from the background as the ultimate source of detector noise. In such a case the detector noise power density is described using the laws of photon rate and detector quantum efficiency. When the number of incoming (target) photons is small in comparison to the number of background photons the approaches are equivalent, since BLIP D* is determined by background photon rate. If the number of target photons is larger than the average number of background photons though, the noise due to the random arrival time of target photons dominates and D* then is meaningless. This case is the unusual one.

Image forming scanners are not usually designed to respond to an absolute radiance level, i.e. not for a dc response. They are designed to follow changes in radiance as the field of view is scanned. This includes gradual changes in the radiance level corresponding to low frequencies. DC restoration can be used to control the intensity levels at the output. Without this form of automatic gain control (AGC) periods of signal blackout or

saturation would occur due to high 1/f noise and amplifier drift at low frequencies.

The signal of interest from the scene is the variation in irradiance H caused by the variation in temperature or emissivity of objects in the scene and may be expressed as:

$$\Delta H = \left(\frac{\Psi}{\pi}\right)\left(\Delta T\int_0^\infty \frac{\partial W}{\partial T}\, d\lambda + \int_0^\infty \frac{\Delta \epsilon_\lambda}{\epsilon_\lambda} W_\lambda d\lambda\right) \quad \text{in } \frac{\text{Watts}}{\text{cm}^2} \qquad \text{(Eq. 6.1)}$$

where Ψ = instantaneous field of view in steradians

T = temperature in degrees Kelvin

ϵ_λ = emissivity (wavelength dependent)

W_λ = spectral radiant emittance in W/cm^2

If most noise in the system is caused by the detector, it may be expressed in terms of "noise equivalent flux density" (NEFD). This is the minimum signal irradiance capable of producing a peak signal to rms noise ratio (S_P/N_R) of one.

The ultimate goal is to find the actual signal-to-noise ratio (S/N) generated by the scanner. This is given as:

$$\frac{S}{N} = \frac{\text{Variation of irradiance in scene } (\Delta H)}{\text{NEFD}} \text{ in Watts} \qquad \text{(Eq. 6.2)}$$

The noise equivalent power (NEP) in watts of the system can be obtained from the figure of merit of the detector (D^*) and is expressed as:

$$NEP = \frac{\sqrt{A_d \cdot \Delta f}}{D^*} \quad \text{in Watts} \qquad \text{(Eq. 6.3)}$$

where A_d = area of the detector in cm^2

Δf = system noise bandwidth

D^* = detector figure of merit in $cm \cdot Hz^{1/2}/watt$

The signal power on the detector is equal to the optical collector area times the signal flux density. Therefore the system noise equivalent flux density is:

$$NEFD = \frac{4\sqrt{A_d \cdot \Delta f}}{\pi D_o^2 D^* \epsilon_o} \quad \text{in Watts/cm}^2 \qquad \text{(Eq. 6.4)}$$

where D_o = diameter of the aperture of the optical system

ϵ_o = optical efficiency

The difference in temperature and emissivities (ΔT and $\Delta \epsilon$) of objects in the scene contribute to the differential radiant emittance (ΔH), but due to the small contribution of $\Delta \epsilon$ for non-BLIP detector operation, its term in equation 6.1 is commonly neglected. By substituting W_ϕ for the first integral term the abbreviated value for radiant emittance becomes then:

$$\Delta H = \frac{\Psi \cdot \Delta T W_\phi}{\pi} \quad \text{in Watts/cm}^2 \qquad \text{(Eq. 6.5)}$$

The instantaneous field of view Ψ is defined by the detector area A_d and the focal length fl as:

$$\Psi = \frac{A_d}{(fl)^2} \quad \text{in steradians} \qquad \text{(Eq. 6.6)}$$

By substituting equation 6.6 into equation 6.4 the noise equivalent flux density is reestablished as:

$$NEFD = \frac{4F\sqrt{w \cdot \Delta f}}{\pi D_o D^* \epsilon_o} \quad \text{in Watts/cm}^2 \qquad \text{(Eq. 6.7)}$$

where F is the f-number of the optics.

The signal-to-noise ratio generated by the scanning system is then (from equation 6.2):

$$\frac{S}{N} = \frac{\Delta T W_\lambda D_o D^* \epsilon_o \sqrt{w}}{4F\sqrt{\Delta f}} \qquad \text{(Eq. 6.8)}$$

Some careful considerations are in order here since the ΔH actually seen by the sensor is modified by the transmittance of the optical components and the atmosphere as discussed earlier. If the bandwidth considered is sufficiently narrow, transmittance losses may be compensated for by using the average transmittance values for each while still producing accurate results. The narrow bandwidth was the premise for the development of transmittance modelling in Chapter IV.

Sensitivity of an image forming scanner is expressed by its noise equivalent temperature (NET). This parameter refers to the temperature difference ΔT within a scene element (with a given emissivity and average temperature of e.g. 300°K) which can produce a change in the electrical signal level equal to the rms system noise. The noise in a well designed system is mostly detector noise. By

incorporating the atmospheric transmittance into equation 6.8 and solving for ΔT, the NET is obtained as:

$$NET = \frac{4F\sqrt{\Delta f}}{\pi D_o D^* \epsilon_o \tau_a W_\beta} \quad \text{in } ^\circ K \qquad \text{(Eq. 6.9)}$$

This an expression of the sensitivity of the detector system as a whole. It makes the assumption that the scene area over which the temperature difference ΔT occurs is much larger than the field of view.

From the design aspect a major emphasis must be placed on the value of D^* for a given detector since its value may vary as much as four orders of magnitude among common detector materials [Ref 2: Table 7.1]. In addition, the D^* of a particular detector will vary considerably from the published data owing to such factors as manufacturing process, electrical bias, cooling, loading, aging and aerodynamic heating of the optical window.

The electrical bandwidth (Δf) of the system is determined by the scan rate. It is proportional to the reciprocal of the dwell time of an image point on the scanning detector surface. The amplifiers connected to the detector can be optimized to obtain a maximum signal-to-noise ratio, especially if the characteristics of the signal and noise are known. In this fashion a number of target/object discrimination techniques may be devised. Optimum filter design is extremely difficult to perform

using only a few components, though a simple band-pass filter with a flat response and a low and high frequency cutoff is often adequate. The very high signal to noise ratios realized by using matched filter (correlation) techniques for processing are virtually impossible due to the passive nature of the systems, but by tweaking the high and low frequency roll-off a much improved background control and target definition may be accomplished with only a slight reduction of the S/N ratio.

If a total field of view of Ω steradians is scanned at a constant rate without redundancy and with an instantaneous field of view Ψ steradians, then the scan is completed in a frame time of t_s. The dwell time t_d of a point on the detector is then $t_s \cdot \Psi/\Omega$. As the total field of view is increased (either in azimuth, elevation or both) linearity in scan rate is difficult to achieve [Ref 4:pp 735]. The off-center loss in dwell time must be compensated for by a scan efficiency factor ϵ_s. As the scan efficiency decreases, an increased electrical bandwidth is required. In this case the optimum bandwidth required is approximately:

$$\Delta f_n = \frac{3\Omega\epsilon_s}{4\Psi t_s} \quad \text{in Hz} \qquad \text{(Eq. 6.10)}$$

Actually this refers to the upper cutoff frequency since it is not practical to design for dc response. The lower

cutoff frequency can usually be designed to handle down to a few Hertz which allows reproduction of at least most of the low frequency features in the scene. If a linear (vertical usually) array of detectors is used, with N elements in the array, then Δf_n can be reduced proportionately.

Equivalent noise bandwidth Δf will usually be larger than required bandwidth Δf_n because of the inherent 1/f noise, amplifier noise, and R-C filter roll-off. In terms of scan rate, the noise equivalent temperature of a scan system is:

$$NET = \left(\frac{1}{w}\right)\left(\frac{\Omega}{t_s}\right)\left(\frac{F}{D_o D^* W_\phi N}\right)\left(\frac{2\ 3\epsilon_s}{\epsilon_o \tau_a}\right) \text{ in } ^\circ K \qquad \text{(Eq. 6.11)}$$

By breaking equation 6.11 into the above groups the corresponding components may be individually analyzed. The first group represents system performance requirements. The second group represents mostly the physical components available at design inception, and the third group represents efficiency parameters of materials used and the atmosphere.

The principles of detectors and line scanning systems are covered extensively in References [2] and [3]. The basics presented thus far will serve as a conceptual approach to modelling seeker systems, and will serve as a baseline for devising discrimination techniques in the modelling process. Based on discussion thus far no

committment has been made with regards to any particular system, but either conceived or existing seekers which use the line scanner techniques operate under the previously explained principles.

1. Filtering for Discrimination

There are three filtering methods which may be used in seeker system designs. These are: 1) Spectral, 2) Spatial, and 3) Temporal. Each method has its physical limitations for implementation in discrimination as will be discussed shortly. In contrast, the incorporation of discrimination into IR seekers leads to the necessity to analyze present countermeasures for possible enhancement to subjugate any of these discrimination techniques.

a. Spectral Filtering

Since background radiant intensity is a primary consideration to seeker design, methods to reduce it are a necessity. Background radiant intensity typically has peaks (maxima) at approximately 0.5 and 10 micrometers caused by solar reflection and thermal self-emission respectively. Around 3 microns a region of minimum background radiance exists. Coincidentally, between the two maxima, most hot targets produce their peak radiant intensity. The simplest method of detection is to examine typical target spectral

characteristics, select a detector most appropriate for operation at the target's peak spectral points, and then use filtering to prevent the background radiant energy from entering the system. If the target of interest exhibits significant wavelength-dependent emissions, one method of discrimination could be the use of notch (2-color spectral bandpass) filters to select specific wavebands. If the radiant energy in the passbands produced by the decoy is then less than that produced by the target (W/sr), the decoy may be rendered ineffective in the seduction role. Thus much of the design of a decoy revolves around matching its spectral radiance to that of the ship it is being designed to protect.

Most IR decoys are omni-directional by nature, and exhibit the same spectral signature in all directions (disregarding wind or sea-surface effects if floating). Target signatures are aspect dependent (intensity) as well as spectrally dependent. As the aspect changes, so does the intensity of certain spectral components. The inherent variability of target signatures in this respect makes it exceedingly difficult to establish discrimination techniques since look-up tables and matched filter methods cannot be used.

b. Temporal Filtering

Spatial frequencies produce time varying signals with a frequency content equal to the spatial frequency times the angular scan rate. In processing then, low frequency rejection and high frequency peaking can be used to eliminate background clutter. Only if the target and background signals can be adequately described can a spatial filter maximize the ratio of target signal to background signal. If multi-element detectors are used, simpler filter techniques are possible. The instantaneous field would be made as small as practical, and the upper frequency cutoff of the electrical filter is selected to correspond to the dwell time of a point on the detector. The low frequency cutoff is usually set at 1/3 to 1/4 of the upper cutoff frequency to block the background radiance without allowing saturation at the other end of the bandpass. This filtering technique is most often used to decrease the probability of false alarms through scan-to-scan comparisons and has little merit in discerning targets from decoys.

c. Spatial Filtering

A more promising approach to discrimination by the seeker may be to process spatial characteristics of the scene. When the range from the seeker to the target is large, the objects in the scene will appear as point

sources. As this range decreases, however, large objects form a distribution within the scene (both horizontal and vertical) while small objects retain their point source characteristics. By keeping the instantaneous field of view small, integral (in spatial sense) processing could be used to discern large distributed objects from small ones. It then becomes the task of the decoy designer to not only make the decoy more intense spectrally than the ship, but to make the signature more widely distributed to simulate large targets. If the decoy is suspended in the air, for example by parachute (and somewhat less so if the decoy is waterborne), the wind will tend to distribute the heat over a wider area; but variable wind conditions and short hang times of parachute-deployed decoys make this method of deployment less attractive than water-borne placement. Some of the effects of wind for signature expansion are still present with water-borne decoys. In addition to the torch emission above the sea surface there exists a reflective component off the sea surface referred to as the "Halo effect" [Ref. 4]. This effect was originally noticed by personnel from Naval Research Laboratory taking infrared measurements of the USS Ticonderoga's signature in both the 3-5 and 8-14 micron bands. The halo effect may readily be seen in Figure 6-1. Upon investigation it was established that the sea foam caused by a white-capped sea surface has very high reflectance at low grazing angles in both infrared

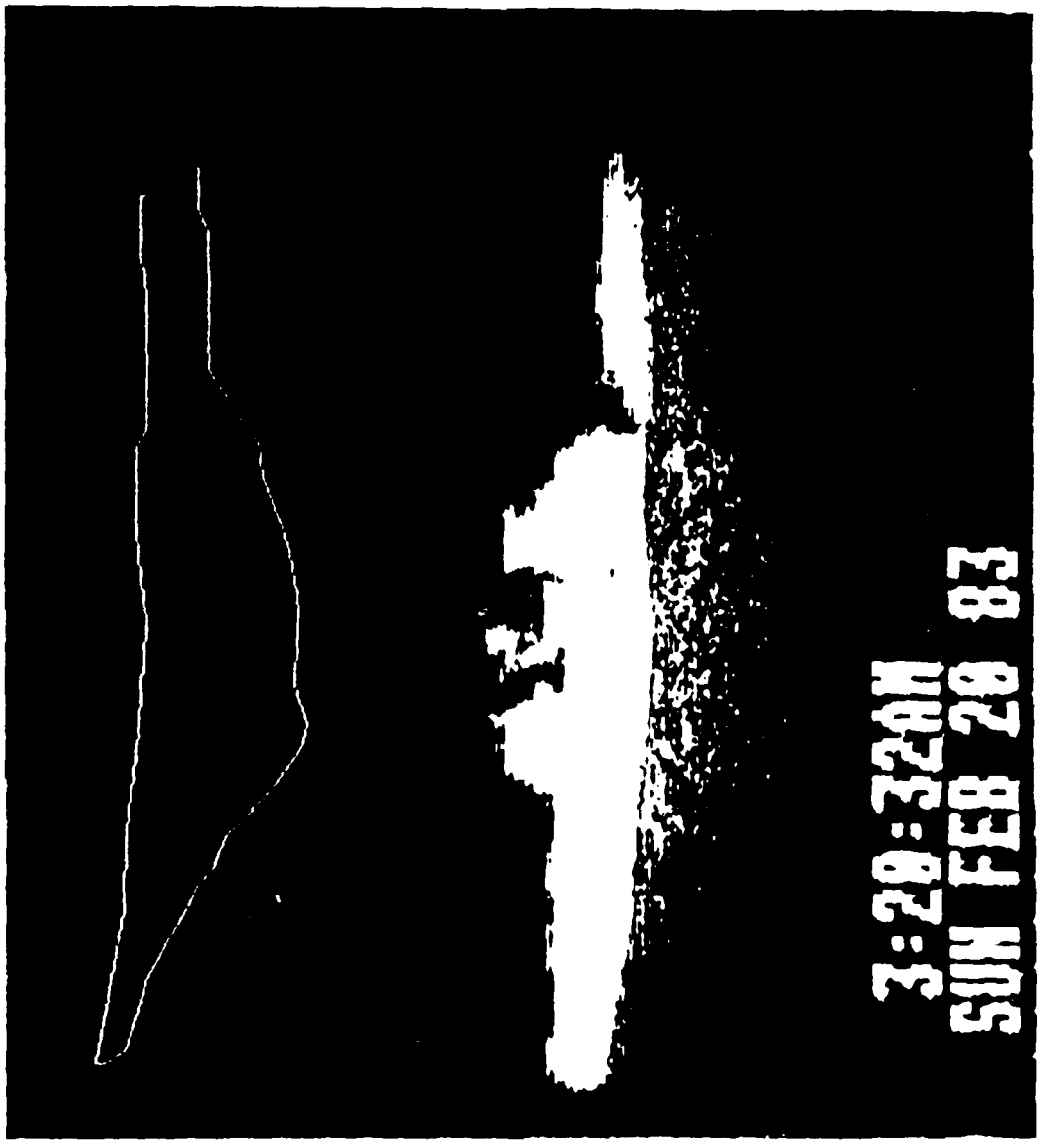

Figure 6-1. Haloing caused by sea-surface reflection around USS Ticonderoga.

bands. The white-caps may be caused by wind, ship movement, and other surface turbulence. When viewed from certain angles as in Figure 6-2, energy from the source which was not originally emitted in the direction of the seeker (observer) is reflected from the sea surface toward the seeker, adding to the original signature radiant density.

From the decoy design aspect this effect may be capitalized upon by incorporating a means of disturbing (foaming) the sea surface over a wide area around a water-borne decoy beneath its burning source. By floating the decoy at the proper height above the foamed sea surface a very large reflective signature may be achieved in addition to the intense point source of the torch itself.

Foaming may be accomplished in many ways, but primary interest must be in distributing over as large an area as possible. Since it is difficult to foam the sea surface over a wide area using a simple squirrel-cage fan or compressed air (too many cylinders) another prospect must be taken which considers weight and space restrictions of the decoy. Foaming of sea water is purely transient and very short in duration, so the above methods would probably be discarded upon testing. The alternate means suggested here is to use a small pneumatically driven suction pump with a mixing chamber to mix the incoming sea water with, for example, light-water or aqueous film-forming foam (AFFF). The mixture may then be sprayed from the decoy by fan or

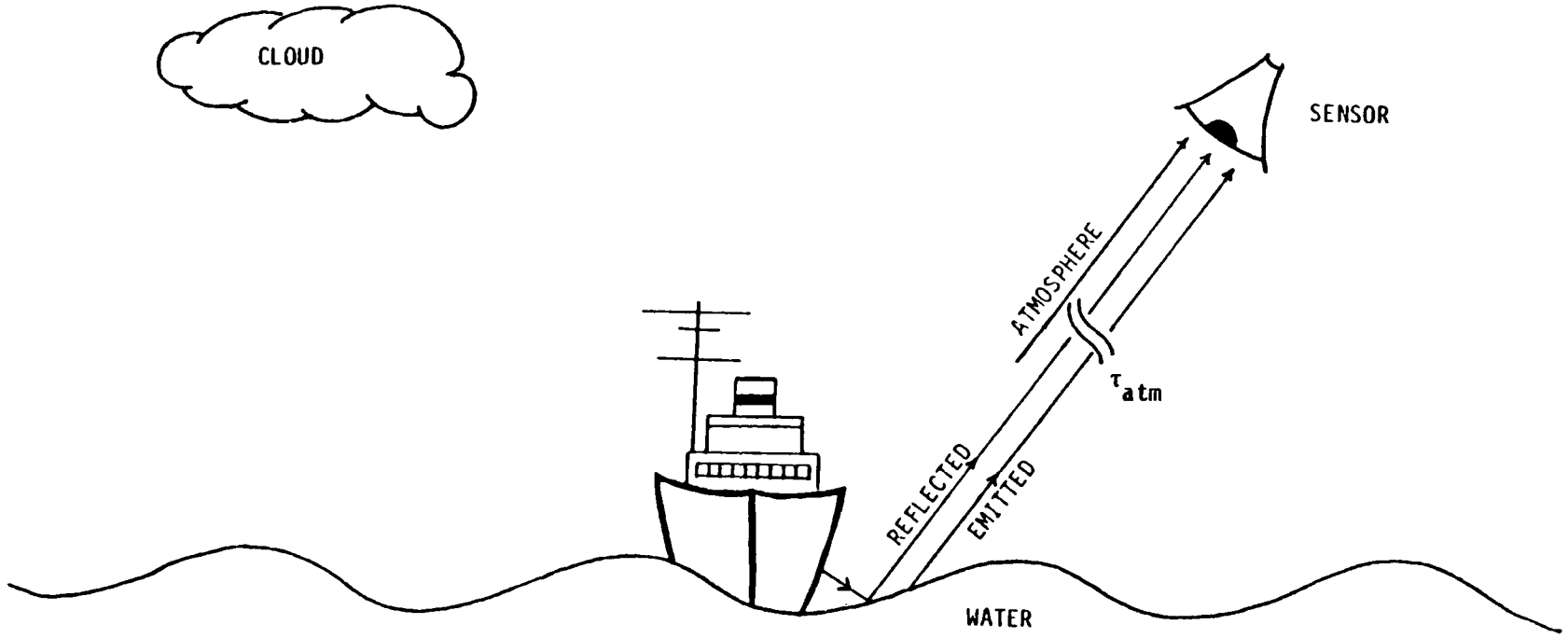

Schematic of contributions of halo signature

Figure 6-2. Geometry of halo caused by reflection

nozzles over a wide area of the sea surface to create a highly reflective layer (using sea surface turbulence for wide angular reflection) and correspondingly large signature. The components in this case could be very inexpensive. Additionally, this technique would work in all infrared bands and, because of the difficulty in devising passive-only discrimination methods, may be the optimum offboard countermeasure to IR seekers. The methods discussed here have not been attempted, but these and many other approaches will need to be addressed in order to meet the IR threat with inexpensive offboard countermeasures.

- TABLE A.1.a -

TRANSMITTANCE IN 3.5 UM BAND - TROPICAL PROFILE
*** LOWTRAN DATA ***

	Range in Km	Visibility in Kilometers 40	30	20	15	10	5
Wind=0	0.20	93.17%	93.14%	93.07%	93.01%	92.88%	92.50%
	1.00	82.05%	81.91%	81.63%	81.35%	80.80%	79.10%
	2.00	73.19%	72.95%	72.46%	71.97%	70.99%	68.16%
	4.00	60.33%	59.92%	59.11%	58.30%	56.73%	52.28%
	8.00	43.64%	43.06%	41.90%	40.77%	38.59%	32.77%
	12.00	32.70%	32.09%	30.81%	29.58%	27.27%	21.40%
	18.00	22.12%	21.46%	20.18%	18.98%	16.77%	11.61%
	21.00	18.45%	17.86%	16.64%	15.50%	13.45%	8.80%
Wind=5	0.20	92.16%	91.75%	90.93%	90.11%	88.49%	83.82%
	1.00	77.70%	75.99%	72.64%	69.42%	63.40%	48.37%
	2.00	65.70%	62.79%	57.39%	52.40%	43.71%	25.45%
	4.00	48.50%	44.39%	37.07%	30.91%	21.50%	7.28%
	8.00	28.30%	23.63%	16.48%	11.46%	5.55%	0.64%
	12.00	17.10%	13.05%	7.60%	4.40%	1.50%	0.06%
	18.00	8.30%	5.56%	2.47%	1.09%	0.21%	0.03%
	21.00	5.90%	3.70%	1.44%	0.55%	0.08%	.00%
Wind=10	0.20	91.76%	91.47%	90.49%	89.52%	87.61%	82.14%
	1.00	76.84%	74.83%	70.92%	67.19%	60.31%	43.70%
	2.00	64.21%	60.88%	54.70%	49.10%	39.56%	20.78%
	4.00	46.41%	41.73%	33.68%	27.13%	17.61%	48.60%
	8.00	25.83%	20.88%	13.60%	8.83%	3.72%	0.28%
	12.00	14.90%	10.84%	5.70%	2.98%	0.82%	0.02%
	18.00	6.80%	4.21%	1.61%	0.61%	0.09%	0.01%
	21.00	4.67%	2.67%	0.87%	0.28%	0.03%	.00%
Wind=15	0.20	91.90%	91.39%	90.37%	89.36%	87.37%	81.69%
	1.00	76.61%	74.51%	70.46%	66.59%	59.49%	42.51%
	2.00	63.81%	60.37%	53.98%	48.22%	38.49%	19.65%
	4.00	45.85%	41.03%	32.80%	26.17%	16.68%	4.35%
	8.00	25.21%	20.19%	12.91%	8.22%	3.33%	0.23%
	12.00	14.38%	10.30%	5.27%	2.68%	0.69%	0.00%
	18.00	6.43%	3.90%	1.43%	0.52%	0.07%	0.00%
	21.00	4.38%	2.45%	0.76%	0.23%	0.02%	0.00%
Wind=20	0.20	91.87%	91.35%	90.32%	89.28%	87.26%	81.47%
	1.00	76.50%	74.36%	70.24%	66.31%	59.11%	41.96%
	2.00	63.62%	60.12%	53.65%	47.82%	38.00%	19.15%
	4.00	45.59%	40.71%	32.40%	25.74%	16.25%	4.13%
	8.00	24.92%	19.87%	12.59%	7.95%	3.17%	0.20%
	12.00	14.08%	10.03%	5.08%	2.55%	0.64%	0.01%
	18.00	6.27%	3.77%	1.35%	0.48%	0.06%	0.01%
	21.00	4.23%	2.33%	0.71%	0.21%	0.02%	.00%

- TABLE A.1.b -

TRANSMITTANCE IN 3.5 UM BAND - TROPICAL PROFILE
*** EMPIRICAL ***

	Range in Km	Visibility in Kilometers 40	30	20	15	10	5
Wind= 0	0.2	86.63%	86.58%	86.57%	86.49%	86.33%	86.03%
Wind= 0	1.0	81.37%	81.13%	81.08%	80.72%	79.94%	78.60%
Wind= 0	2.0	75.25%	74.80%	74.70%	74.05%	72.63%	70.20%
Wind= 0	4.0	64.34%	63.59%	63.41%	62.31%	59.94%	56.01%
Wind= 0	8.0	47.04%	45.95%	45.69%	44.12%	40.82%	35.64%
Wind= 0	12.0	34.40%	33.20%	32.93%	31.24%	27.80%	22.68%
Wind= 0	18.0	21.50%	20.39%	20.14%	18.61%	15.63%	11.52%
Wind= 0	21.0	17.00%	15.98%	15.75%	14.36%	11.72%	8.21%
Wind= 5	0.2	85.75%	85.14%	84.16%	83.06%	80.76%	74.54%
Wind= 5	1.0	77.30%	74.60%	70.42%	65.94%	57.28%	38.36%
Wind= 5	2.0	67.91%	63.23%	56.35%	49.41%	37.29%	16.72%
Wind= 5	4.0	52.40%	45.44%	36.08%	27.74%	15.80%	3.18%
Wind= 5	8.0	31.21%	23.46%	14.79%	8.74%	2.84%	0.11%
Wind= 5	12.0	18.58%	12.11%	6.07%	2.76%	0.51%	0.00%
Wind= 5	18.0	8.54%	4.49%	1.59%	0.49%	0.04%	0.00%
Wind= 5	21.0	5.79%	2.74%	0.82%	0.21%	0.01%	0.00%
Wind=10	0.2	85.55%	84.88%	83.82%	82.63%	80.13%	73.41%
Wind=10	1.0	76.39%	73.48%	69.00%	64.22%	55.08%	35.56%
Wind=10	2.0	66.32%	61.35%	54.10%	46.87%	34.47%	14.37%
Wind=10	4.0	49.98%	42.77%	33.26%	24.96%	13.50%	2.35%
Wind=10	8.0	28.38%	20.79%	12.57%	7.08%	2.07%	0.06%
Wind=10	12.0	16.12%	10.10%	4.75%	2.01%	0.32%	0.00%
Wind=10	18.0	6.90%	3.42%	1.10%	0.30%	0.02%	0.00%
Wind=10	21.0	4.51%	1.99%	0.53%	0.12%	0.00%	0.00%
Wind=15	0.2	85.50%	84.82%	83.74%	82.53%	79.99%	73.16%
Wind=15	1.0	76.19%	73.23%	68.68%	63.84%	54.60%	34.96%
Wind=15	2.0	65.97%	60.94%	53.61%	46.32%	33.87%	13.89%
Wind=15	4.0	49.45%	42.19%	32.66%	24.38%	13.04%	2.19%
Wind=15	8.0	27.79%	20.23%	12.12%	6.75%	1.93%	0.05%
Wind=15	12.0	15.61%	9.70%	4.50%	1.87%	0.29%	0.00%
Wind=15	18.0	6.58%	3.22%	1.02%	0.27%	0.02%	0.00%
Wind=15	21.0	4.27%	1.86%	0.48%	0.10%	0.00%	0.00%
Wind=20	0.2	85.49%	84.81%	83.73%	82.51%	79.96%	73.11%
Wind=20	1.0	76.15%	73.17%	68.61%	63.76%	54.49%	34.83%
Wind=20	2.0	65.89%	60.84%	53.50%	46.19%	33.74%	13.78%
Wind=20	4.0	49.33%	42.07%	32.52%	24.25%	12.94%	2.16%
Wind=20	8.0	27.66%	20.11%	12.02%	6.68%	1.90%	0.05%
Wind=20	12.0	15.50%	9.61%	4.44%	1.84%	0.28%	0.00%
Wind=20	18.0	6.51%	3.18%	1.00%	0.27%	0.02%	0.00%
Wind=20	21.0	4.22%	1.83%	0.47%	0.10%	0.00%	0.00%

- TABLE A.2.a -

TRANSMITTANCE IN 3.5 UM BAND - MIDLATITUDE SUMMER PROFILE
*** LOWTRAN DATA ***

	Range in Km	Visibility in Kilometers 40	30	20	15	10	5
Wind=0	0.20	94.16%	94.12%	94.06%	94.00%	93.87%	93.49%
	1.00	84.47%	84.33%	84.05%	83.76%	83.20%	81.53%
	2.00	76.79%	76.53%	76.02%	75.51%	74.49%	71.53%
	4.00	65.59%	65.16%	64.28%	63.42%	61.72%	56.92%
	8.00	50.26%	49.59%	48.27%	46.98%	44.50%	37.84%
	12.00	39.82%	39.03%	37.48%	35.99%	33.17%	26.02%
	18.00	28.86%	28.01%	26.36%	24.79%	21.94%	15.24%
	21.00	24.90%	24.04%	22.40%	20.86%	18.09%	11.82%
Wind=5	0.20	93.14%	92.72%	91.89%	91.06%	89.43%	84.72%
	1.00	80.01%	78.24%	74.80%	71.48%	65.29%	49.83%
	2.00	68.89%	65.88%	60.21%	54.99%	45.88%	26.72%
	4.00	52.78%	48.28%	40.33%	33.64%	23.41%	7.94%
	8.00	32.55%	27.23%	19.00%	13.22%	6.40%	0.74%
	12.00	20.75%	15.88%	9.26%	5.37%	1.81%	0.07%
	18.00	10.86%	7.27%	3.23%	1.43%	0.28%	0.00%
	21.00	7.96%	4.98%	1.94%	0.75%	0.11%	0.00%
Wind=10	0.20	92.93%	92.44%	91.45%	90.47%	88.53%	83.01%
	1.00	79.11%	77.04%	73.02%	69.18%	62.10%	45.00%
	2.00	67.35%	63.86%	57.38%	51.50%	41.50%	21.79%
	4.00	50.46%	45.37%	36.62%	29.50%	19.15%	5.28%
	8.00	29.74%	24.05%	15.66%	10.16%	4.29%	0.33%
	12.00	18.13%	13.18%	6.93%	3.62%	0.99%	0.02%
	18.00	8.87%	5.49%	2.09%	0.79%	0.11%	0.00%
	21.00	6.28%	3.60%	1.17%	0.38%	0.04%	0.00%
Wind=15	0.20	92.87%	92.36%	91.33%	90.30%	88.29%	82.55%
	1.00	78.87%	76.71%	72.54%	68.55%	61.25%	43.76%
	2.00	66.94%	63.32%	56.62%	50.58%	40.37%	20.60%
	4.00	49.84%	44.60%	35.66%	28.45%	18.13%	4.72%
	8.00	29.02%	23.24%	14.86%	9.46%	3.84%	0.26%
	12.00	17.47%	12.52%	6.40%	3.25%	0.84%	0.01%
	18.00	8.39%	5.09%	1.86%	0.67%	0.09%	0.00%
	21.00	5.89%	3.29%	1.02%	0.31%	0.03%	0.00%
Wind=20	0.20	92.84%	92.32%	91.27%	90.23%	88.18%	82.33%
	1.00	78.75%	76.56%	72.31%	68.27%	60.85%	43.19%
	2.00	66.74%	63.07%	56.27%	50.15%	39.85%	20.07%
	4.00	49.55%	44.25%	35.22%	27.98%	17.66%	4.48%
	8.00	28.68%	22.87%	14.49%	9.14%	3.65%	0.23%
	12.00	17.17%	12.22%	6.16%	3.09%	0.78%	0.01%
	18.00	8.17%	4.91%	1.76%	0.62%	0.08%	0.00%
	21.00	5.71%	3.15%	0.95%	0.28%	0.03%	0.00%

- TABLE A.2.b -

TRANSMITTANCE IN 3.5 UM BAND - MIDLATITUDE SUMMER PROFILE
*** EMPIRICAL ***

	Range in Km	Visibility in Kilometers 40	30	20	15	10	5
Wind= 0	0.2	86.48%	86.39%	86.35%	86.26%	86.09%	85.79%
Wind= 0	1.0	82.52%	82.07%	81.88%	81.47%	80.65%	79.28%
Wind= 0	2.0	77.82%	76.99%	76.62%	75.86%	74.34%	71.83%
Wind= 0	4.0	69.21%	67.73%	67.09%	65.77%	63.16%	58.96%
Wind= 0	8.0	54.74%	52.43%	51.45%	49.44%	45.60%	39.73%
Wind= 0	12.0	43.30%	40.59%	39.45%	37.16%	32.92%	26.77%
Wind= 0	18.0	30.46%	27.64%	26.49%	24.22%	20.19%	14.81%
Wind= 0	21.0	25.55%	22.81%	21.70%	19.55%	15.81%	11.01%
Wind= 5	0.2	85.70%	85.07%	84.11%	83.02%	80.69%	74.23%
Wind= 5	1.0	78.85%	76.01%	71.83%	67.29%	58.34%	38.46%
Wind= 5	2.0	71.06%	66.03%	58.97%	51.74%	38.89%	16.90%
Wind= 5	4.0	57.70%	49.83%	39.74%	30.60%	17.29%	3.26%
Wind= 5	8.0	38.05%	28.38%	18.05%	10.70%	3.42%	0.12%
Wind= 5	12.0	25.10%	16.16%	8.20%	3.74%	0.67%	0.00%
Wind= 5	18.0	13.44%	6.95%	2.51%	0.77%	0.06%	0.00%
Wind= 5	21.0	9.84%	4.55%	1.39%	0.35%	0.02%	0.00%
Wind=10	0.2	85.49%	84.79%	83.73%	82.52%	79.93%	72.83%
Wind=10	1.0	77.90%	74.78%	70.20%	65.26%	55.65%	34.95%
Wind=10	2.0	69.36%	63.90%	56.32%	48.67%	35.39%	13.96%
Wind=10	4.0	54.97%	46.67%	36.25%	27.08%	14.32%	2.23%
Wind=10	8.0	34.54%	24.90%	15.02%	8.38%	2.34%	0.06%
Wind=10	12.0	21.70%	13.28%	6.22%	2.59%	0.38%	0.00%
Wind=10	18.0	10.81%	5.17%	1.66%	0.45%	0.03%	0.00%
Wind=10	21.0	7.63%	3.23%	0.86%	0.19%	0.01%	0.00%
Wind=15	0.2	85.44%	84.72%	83.63%	82.39%	79.73%	72.47%
Wind=15	1.0	77.66%	74.46%	69.78%	64.75%	54.97%	34.09%
Wind=15	2.0	68.92%	63.36%	55.65%	47.91%	34.54%	13.28%
Wind=15	4.0	54.29%	45.89%	35.40%	26.23%	13.63%	2.02%
Wind=15	8.0	33.68%	24.06%	14.32%	7.86%	2.12%	0.05%
Wind=15	12.0	20.90%	12.62%	5.79%	2.36%	0.33%	0.00%
Wind=15	18.0	10.21%	4.79%	1.49%	0.39%	0.02%	0.00%
Wind=15	21.0	7.14%	2.95%	0.76%	0.16%	0.01%	0.00%
Wind=20	0.2	85.42%	84.70%	83.60%	82.35%	79.68%	72.37%
Wind=20	1.0	77.59%	74.38%	69.68%	64.61%	54.80%	33.87%
Wind=20	2.0	68.81%	63.23%	55.48%	47.71%	34.32%	13.11%
Wind=20	4.0	54.11%	45.68%	35.18%	26.02%	13.46%	1.96%
Wind=20	8.0	33.46%	23.85%	14.15%	7.74%	2.07%	0.04%
Wind=20	12.0	20.70%	12.45%	5.69%	2.30%	0.32%	0.00%
Wind=20	18.0	10.06%	4.70%	1.45%	0.37%	0.02%	0.00%
Wind=20	21.0	7.02%	2.89%	0.73%	0.15%	0.00%	0.00%

- TABLE A.3.a -

TRANSMITTANCE IN 3.5 UM BAND - MIDLATITUDE WINTER PROFILE
*** LOWTRAN DATA ***

	Range in Km	Visibility in Kilometers 40	30	20	15	10	5
Wind=0	0.2	97.55%	97.52%	97.45%	97.39%	97.26%	96.86%
	1.00	92.46%	92.30%	91.99%	91.68%	91.06%	89.22%
	2.00	88.34%	88.04%	87.45%	86.85%	85.68%	82.26%
	4.00	82.24%	81.69%	80.59%	79.50%	77.36%	71.32%
	8.00	73.25%	72.28%	70.35%	68.45%	64.82%	55.09%
	12.00	66.20%	64.88%	62.30%	59.80%	55.10%	43.18%
	18.00	57.51%	55.80%	52.51%	49.38%	43.68%	30.29%
	21.00	53.76%	51.90%	48.34%	45.00%	39.00%	25.45%
Wind=5	0.2	96.50%	96.07%	95.21%	94.35%	92.66%	87.78%
	1.00	87.57%	85.64%	81.88%	78.25%	71.47%	54.55%
	2.00	79.25%	75.79%	69.27%	63.27%	52.78%	30.75%
	4.00	66.19%	60.54%	50.58%	42.18%	29.36%	9.96%
	8.00	47.45%	39.69%	27.70%	19.27%	9.34%	1.08%
	12.00	34.51%	26.40%	15.40%	8.93%	3.01%	0.12%
	18.00	21.65%	14.49%	6.45%	2.85%	0.56%	0.00%
	21.00	17.19%	10.76%	4.19%	1.62%	0.24%	0.00%
Wind=10	0.2	96.28%	95.77%	94.75%	93.73%	91.72%	85.99%
	1.00	86.58%	84.31%	79.90%	75.69%	67.94%	49.21%
	2.00	77.47%	73.45%	65.98%	59.21%	47.69%	25.02%
	4.00	63.24%	56.86%	45.87%	36.94%	23.97%	6.60%
	8.00	43.32%	35.01%	22.79%	14.78%	6.22%	0.47%
	12.00	30.11%	21.87%	11.49%	6.00%	1.64%	0.03%
	18.00	17.64%	10.92%	4.16%	1.57%	0.22%	0.00%
	21.00	13.54%	7.74%	2.51%	0.81%	0.08%	0.00%
Wind=15	0.2	96.22%	95.69%	94.62%	93.56%	91.47%	85.51%
	1.00	86.31%	83.95%	79.37%	75.01%	67.00%	47.83%
	2.00	76.98%	72.82%	65.10%	58.13%	46.38%	23.64%
	4.00	62.46%	55.88%	44.66%	35.62%	22.67%	5.89%
	8.00	42.25%	33.82%	21.60%	13.74%	5.57%	0.38%
	12.00	29.00%	20.77%	10.60%	5.38%	1.39%	0.02%
	18.00	16.68%	10.11%	3.69%	1.33%	0.17%	0.00%
	21.00	12.68%	7.07%	2.18%	0.66%	0.06%	0.00%
Wind=20	0.2	96.19%	95.65%	94.56%	93.48%	91.35%	85.28%
	1.00	86.19%	83.78%	79.12%	74.69%	66.56%	47.20%
	2.00	76.76%	72.52%	64.69%	57.64%	45.78%	23.02%
	4.00	62.09%	55.43%	44.10%	35.01%	22.09%	5.59%
	8.00	41.76%	33.28%	21.07%	13.28%	5.28%	0.34%
	12.00	28.49%	20.27%	10.21%	5.11%	1.28%	0.02%
	18.00	16.24%	9.75%	3.48%	1.23%	0.16%	0.00%
	21.00	12.30%	6.78%	2.04%	0.61%	0.05%	0.00%

- TABLE 4.3.b -

TRANSMITTANCE IN 3.5 UM BAND - MIDLATITUDE WINTER PROFILE
*** EMPIRICAL ***

	Range in Km	Visibility in Kilometers 40	30	20	15	10	5
Wind= 0	0.2	93.30%	93.24%	93.23%	93.15%	92.97%	92.65%
Wind= 0	1.0	91.21%	90.93%	90.87%	90.47%	89.59%	88.08%
Wind= 0	2.0	88.66%	88.12%	87.99%	87.22%	85.54%	82.68%
Wind= 0	4.0	83.77%	82.75%	82.52%	81.08%	77.99%	72.85%
Wind= 0	8.0	74.78%	72.98%	72.57%	70.06%	64.82%	56.56%
Wind= 0	12.0	66.76%	64.37%	63.83%	60.54%	53.87%	43.92%
Wind= 0	18.0	56.32%	53.31%	52.64%	48.63%	40.82%	30.05%
Wind= 0	21.0	51.72%	48.52%	47.81%	43.59%	35.53%	24.85%
Wind= 5	0.2	92.32%	91.65%	90.61%	89.09%	85.29%	73.25%
Wind= 5	1.0	86.51%	83.44%	78.80%	72.43%	58.24%	27.21%
Wind= 5	2.0	79.75%	74.19%	66.18%	55.90%	36.15%	7.89%
Wind= 5	4.0	67.79%	58.67%	46.67%	33.31%	13.93%	0.66%
Wind= 5	8.0	48.97%	36.68%	23.22%	11.82%	2.07%	0.00%
Wind= 5	12.0	35.38%	22.94%	11.55%	4.20%	0.31%	0.00%
Wind= 5	18.0	21.73%	11.34%	4.05%	0.89%	0.02%	0.00%
Wind= 5	21.0	17.03%	7.97%	2.40%	0.41%	0.00%	0.00%
Wind=10	0.2	92.09%	91.33%	90.14%	88.41%	84.08%	70.58%
Wind=10	1.0	85.46%	81.98%	76.77%	69.67%	54.22%	22.60%
Wind=10	2.0	77.83%	71.63%	62.81%	51.73%	31.34%	5.44%
Wind=10	4.0	64.57%	54.68%	42.04%	28.52%	10.46%	0.32%
Wind=10	8.0	44.43%	31.87%	18.83%	8.67%	1.17%	0.00%
Wind=10	12.0	30.57%	18.57%	8.44%	2.63%	0.13%	0.00%
Wind=10	18.0	17.45%	8.26%	2.53%	0.44%	0.00%	0.00%
Wind=10	21.0	13.18%	5.51%	1.39%	0.18%	0.00%	0.00%
Wind=15	0.2	92.04%	91.26%	90.03%	88.25%	83.81%	69.99%
Wind=15	1.0	85.22%	81.65%	76.31%	69.05%	53.34%	21.66%
Wind=15	2.0	77.40%	71.06%	62.06%	50.82%	30.33%	5.00%
Wind=15	4.0	63.85%	53.81%	41.04%	27.53%	9.80%	0.27%
Wind=15	8.0	43.45%	30.86%	17.95%	8.07%	1.02%	0.00%
Wind=15	12.0	29.57%	17.70%	7.85%	2.37%	0.11%	0.00%
Wind=15	18.0	16.60%	7.69%	2.27%	0.38%	0.00%	0.00%
Wind=15	21.0	12.43%	5.06%	1.22%	0.15%	0.00%	0.00%
Wind=20	0.2	92.03%	91.24%	90.01%	88.21%	83.75%	69.85%
Wind=20	1.0	85.17%	81.58%	76.20%	68.91%	53.15%	21.45%
Wind=20	2.0	77.30%	70.92%	61.89%	50.61%	30.10%	4.91%
Wind=20	4.0	63.69%	53.61%	40.82%	27.30%	9.66%	0.26%
Wind=20	8.0	43.23%	30.63%	17.76%	7.94%	0.99%	0.00%
Wind=20	12.0	29.34%	17.50%	7.73%	2.31%	0.10%	0.00%
Wind=20	18.0	16.41%	7.56%	2.22%	0.36%	0.00%	0.00%
Wind=20	21.0	12.27%	4.97%	1.19%	0.14%	0.00%	0.00%

- TABLE A.4.a -

TRANSMITTANCE IN 3.5 UM BAND - SUB-ARCTIC SUMMER PROFILE
*** LOWTRAN DATA ***

	Range in Km	Visibility in Kilometers 40 Km	30 Km	20 Km	15 Km	10 Km	5 Km
Wind=0	0.20	95.52%	95.49%	95.43%	95.36%	95.23%	94.85%
	1.00	87.64%	87.49%	87.20%	86.91%	86.32%	84.60%
	2.00	81.41%	81.14%	80.60%	80.05%	78.98%	75.86%
	4.00	72.23%	71.75%	70.79%	69.84%	67.98%	62.72%
	8.00	59.00%	58.22%	56.68%	55.17%	52.26%	44.48%
	12.00	49.49%	48.51%	46.60%	44.74%	41.26%	32.40%
	18.00	38.90%	37.75%	35.54%	33.44%	29.61%	20.60%
	21.00	34.70%	33.50%	31.23%	29.09%	25.24%	16.53%
Wind=5	0.20	94.49%	94.07%	93.23%	92.38%	90.73%	85.95%
	1.00	83.00%	81.17%	77.60%	74.16%	67.73%	51.69%
	2.00	73.02%	69.84%	63.83%	58.29%	48.63%	28.32%
	4.00	58.11%	53.15%	44.40%	37.03%	25.77%	8.74%
	8.00	38.19%	31.95%	22.30%	15.51%	7.51%	0.86%
	12.00	25.78%	19.72%	11.50%	6.67%	2.25%	0.09%
	18.00	14.62%	9.79%	4.36%	1.92%	0.38%	0.00%
	21.00	11.08%	6.93%	2.70%	1.04%	0.16%	0.00%
Wind=10	0.20	94.28%	93.78%	92.78%	91.79%	89.83%	84.23%
	1.00	82.08%	79.93%	75.77%	71.79%	64.45%	46.73%
	2.00	71.42%	67.72%	60.85%	54.63%	44.03%	23.15%
	4.00	55.58%	49.98%	40.36%	32.52%	21.13%	5.84%
	8.00	34.94%	28.26%	18.42%	11.96%	5.05%	0.39%
	12.00	22.55%	16.40%	8.63%	4.52%	1.24%	0.03%
	18.00	11.97%	7.42%	2.83%	1.07%	0.15%	0.00%
	21.00	8.77%	5.02%	1.63%	0.53%	0.05%	0.00%
Wind=15	0.20	94.22%	93.70%	92.66%	91.62%	89.58%	83.77%
	1.00	81.83%	79.60%	75.28%	71.15%	63.58%	45.46%
	2.00	70.98%	67.16%	60.06%	53.66%	42.85%	21.90%
	4.00	54.91%	49.15%	39.31%	31.38%	20.01%	5.23%
	8.00	34.10%	27.32%	17.48%	11.14%	4.53%	0.31%
	12.00	21.74%	15.59%	7.98%	4.06%	1.05%	0.02%
	18.00	11.33%	6.88%	2.52%	0.91%	0.12%	0.00%
	21.00	8.23%	4.60%	1.42%	0.44%	0.04%	0.00%
Wind=20	0.20	94.20%	93.67%	92.60%	91.55%	89.47%	83.55%
	1.00	81.72%	79.44%	75.05%	70.86%	63.18%	44.87%
	2.00	70.78%	66.89%	59.70%	53.22%	42.31%	21.34%
	4.00	54.60%	48.76%	38.84%	30.86%	19.51%	4.96%
	8.00	33.71%	26.89%	17.06%	10.77%	4.30%	0.28%
	12.00	21.37%	15.23%	7.69%	3.86%	0.97%	0.02%
	18.00	11.04%	6.64%	2.38%	0.85%	0.11%	0.00%
	21.00	7.98%	4.41%	1.34%	0.40%	0.04%	0.00%

- TABLE A.4.b -

TRANSMITTANCE IN 3.5 UM BAND - SUB-ARCTIC SUMMER PROFILE
*** EMPIRICAL ***

	Range in Km	Visibility in Kilometers 40	30	20	15	10	5
Wind= 0	0.2	92.92%	92.87%	92.85%	92.77%	92.59%	92.28%
Wind= 0	1.0	89.38%	89.11%	89.05%	88.66%	87.81%	86.34%
Wind= 0	2.0	85.13%	84.63%	84.51%	83.77%	82.17%	79.44%
Wind= 0	4.0	77.24%	76.33%	76.11%	74.79%	71.96%	67.26%
Wind= 0	8.0	63.59%	62.09%	61.74%	59.62%	55.19%	48.22%
Wind= 0	12.0	52.35%	50.51%	50.08%	47.52%	42.32%	34.57%
Wind= 0	18.0	39.10%	37.06%	36.59%	33.82%	28.43%	20.98%
Wind= 0	21.0	33.79%	31.75%	31.28%	28.53%	23.30%	16.35%
Wind= 5	0.2	91.95%	91.33%	90.33%	89.08%	86.25%	78.02%
Wind= 5	1.0	84.81%	81.96%	77.59%	72.38%	61.59%	37.30%
Wind= 5	2.0	76.65%	71.59%	64.16%	55.83%	40.43%	14.83%
Wind= 5	4.0	62.62%	54.63%	43.88%	33.22%	17.42%	2.34%
Wind= 5	8.0	41.79%	31.80%	20.52%	11.76%	3.23%	0.06%
Wind= 5	12.0	27.89%	18.52%	9.60%	4.17%	0.60%	0.00%
Wind= 5	18.0	15.20%	8.23%	3.07%	0.88%	0.05%	0.00%
Wind= 5	21.0	11.23%	5.48%	1.74%	0.40%	0.01%	0.00%
Wind=10	0.2	91.73%	91.04%	89.93%	88.54%	85.40%	76.34%
Wind=10	1.0	83.80%	80.67%	75.87%	70.20%	58.61%	33.46%
Wind=10	2.0	74.85%	69.35%	61.36%	52.52%	36.61%	11.93%
Wind=10	4.0	59.70%	51.25%	40.12%	29.40%	14.29%	1.52%
Wind=10	8.0	37.99%	28.00%	17.15%	9.21%	2.17%	0.02%
Wind=10	12.0	24.17%	15.29%	7.34%	2.89%	0.33%	0.00%
Wind=10	18.0	12.27%	6.17%	2.05%	0.51%	0.02%	0.00%
Wind=10	21.0	8.74%	3.92%	1.08%	0.21%	0.00%	0.00%
Wind=15	0.2	91.68%	90.97%	89.84%	88.42%	85.21%	75.97%
Wind=15	1.0	83.58%	80.38%	75.50%	69.72%	57.97%	32.66%
Wind=15	2.0	74.45%	68.86%	60.75%	51.81%	35.81%	11.37%
Wind=15	4.0	59.07%	50.53%	39.33%	28.61%	13.67%	1.38%
Wind=15	8.0	37.19%	27.21%	16.48%	8.72%	1.99%	0.02%
Wind=15	12.0	23.41%	14.66%	6.91%	2.66%	0.29%	0.00%
Wind=15	18.0	11.70%	5.79%	1.87%	0.45%	0.02%	0.00%
Wind=15	21.0	8.27%	3.64%	0.98%	0.18%	0.00%	0.00%
Wind=20	0.2	91.67%	90.96%	89.82%	88.39%	85.17%	75.89%
Wind=20	1.0	83.53%	80.32%	75.41%	69.62%	57.82%	32.48%
Wind=20	2.0	74.36%	68.75%	60.61%	51.65%	35.63%	11.24%
Wind=20	4.0	58.93%	50.37%	39.15%	28.43%	13.53%	1.35%
Wind=20	8.0	37.01%	27.04%	16.34%	8.62%	1.95%	0.02%
Wind=20	12.0	23.25%	14.52%	6.82%	2.61%	0.28%	0.00%
Wind=20	18.0	11.57%	5.71%	1.84%	0.44%	0.02%	0.00%
Wind=20	21.0	8.16%	3.58%	0.95%	0.18%	0.00%	0.00%

- TABLE A.5.a -

TRANSMITTANCE IN 3.5 UM BAND - SUB-ARCTIC WINTER PROFILE
*** LOWTRAN DATA ***

	Range in Km	Visibility in Kilometers 40	30	20	15	10	5
Wind=0	0.20	98.73%	98.70%	98.63%	98.56%	98.43%	98.02%
	1.00	95.78%	95.62%	95.29%	94.96%	94.30%	92.38%
	2.00	93.00%	92.68%	92.05%	91.41%	90.15%	86.51%
	4.00	88.76%	88.16%	86.96%	85.76%	83.42%	76.80%
	8.00	82.56%	81.44%	79.23%	77.06%	72.91%	61.81%
	12.00	77.53%	75.96%	72.89%	69.92%	64.34%	50.22%
	18.00	71.13%	68.98%	64.84%	60.92%	53.78%	37.08%
	21.00	68.30%	65.90%	61.31%	57.01%	49.29%	31.94%
Wind=5	0.20	97.67%	97.24%	96.37%	95.50%	93.78%	88.85%
	1.00	90.73%	88.73%	84.83%	81.08%	74.06%	56.54%
	2.00	83.45%	79.81%	72.96%	66.64%	55.60%	32.41%
	4.00	71.47%	65.38%	54.63%	45.57%	31.73%	10.78%
	8.00	53.53%	44.78%	31.27%	21.76%	10.55%	1.22%
	12.00	40.47%	30.98%	18.07%	10.49%	3.54%	0.14%
	18.00	26.83%	17.96%	8.00%	3.54%	0.69%	0.01%
	21.00	21.90%	13.71%	5.34%	2.06%	0.31%	0.00%
Wind=10	0.20	97.44%	96.92%	95.88%	94.84%	92.80%	86.97%
	1.00	89.67%	87.30%	82.71%	78.33%	70.26%	50.81%
	2.00	81.50%	77.26%	69.36%	62.20%	50.05%	26.17%
	4.00	68.18%	61.25%	49.37%	39.71%	25.71%	7.03%
	8.00	48.70%	39.32%	25.54%	16.52%	6.92%	0.52%
	12.00	35.13%	25.48%	13.34%	6.94%	1.88%	0.04%
	18.00	21.70%	13.40%	5.08%	1.91%	0.27%	0.00%
	21.00	17.09%	9.74%	3.14%	1.00%	0.10%	0.00%
Wind=15	0.20	97.38%	96.83%	95.74%	94.66%	92.53%	86.46%
	1.00	89.37%	86.90%	82.13%	77.59%	69.24%	49.32%
	2.00	80.97%	76.56%	68.39%	61.02%	48.61%	24.66%
	4.00	67.29%	60.16%	48.00%	38.22%	24.25%	6.24%
	8.00	47.44%	37.92%	24.14%	15.30%	6.16%	0.41%
	12.00	33.78%	24.13%	12.26%	6.19%	1.58%	0.03%
	18.00	20.45%	12.35%	4.47%	1.60%	0.21%	0.00%
	21.00	15.96%	8.86%	2.71%	0.82%	0.08%	0.00%
Wind=20	0.20	97.35%	96.79%	95.68%	94.58%	92.40%	86.22%
	1.00	89.24%	86.72%	81.86%	77.24%	68.77%	48.64%
	2.00	80.72%	76.24%	67.94%	60.48%	47.94%	23.98%
	4.00	66.88%	59.65%	47.37%	37.54%	23.59%	5.90%
	8.00	46.86%	37.28%	23.51%	14.76%	5.83%	0.36%
	12.00	33.16%	23.53%	11.78%	5.86%	1.46%	0.02%
	18.00	19.90%	11.89%	4.21%	1.48%	0.18%	0.00%
	21.00	15.45%	8.47%	2.53%	0.74%	0.07%	0.00%

- TABLE A.5.b -

TRANSMITTANCE IN 3.5 UM BAND - SUBARCTIC WINTER PROFILE
*** EMPIRICAL ***

	Range in Km	Visibility in Kilometers 40	30	20	15	10	5
Wind= 0	0.2	96.02%	95.96%	95.95%	95.86%	95.68%	95.34%
Wind= 0	1.0	94.69%	94.40%	94.33%	93.91%	92.98%	91.39%
Wind= 0	2.0	93.05%	92.47%	92.34%	91.52%	89.73%	86.67%
Wind= 0	4.0	89.85%	88.74%	88.49%	86.92%	83.55%	77.96%
Wind= 0	8.0	83.78%	81.73%	81.26%	78.41%	72.44%	63.08%
Wind= 0	12.0	78.12%	75.27%	74.63%	70.73%	62.81%	51.03%
Wind= 0	18.0	70.34%	66.52%	65.67%	60.59%	50.71%	37.14%
Wind= 0	21.0	66.74%	62.54%	61.61%	56.09%	45.57%	31.68%
Wind= 5	0.2	95.02%	94.28%	93.17%	91.28%	86.18%	69.38%
Wind= 5	1.0	89.86%	86.39%	81.42%	73.51%	55.13%	18.65%
Wind= 5	2.0	83.80%	77.46%	68.80%	56.08%	31.54%	3.61%
Wind= 5	4.0	72.87%	62.26%	49.12%	32.64%	10.32%	0.14%
Wind= 5	8.0	55.11%	40.23%	25.04%	11.06%	1.11%	0.00%
Wind= 5	12.0	41.68%	26.00%	12.76%	3.75%	0.12%	0.00%
Wind= 5	18.0	27.41%	13.50%	4.65%	0.74%	0.00%	0.00%
Wind= 5	21.0	22.23%	9.73%	2.80%	0.33%	0.00%	0.00%
Wind=10	0.2	94.78%	93.90%	92.60%	90.38%	84.44%	65.34%
Wind=10	1.0	88.72%	84.69%	78.95%	69.96%	49.78%	13.81%
Wind=10	2.0	81.68%	74.43%	64.69%	50.80%	25.71%	1.98%
Wind=10	4.0	69.24%	57.49%	43.43%	26.78%	6.86%	0.04%
Wind=10	8.0	49.76%	34.30%	19.57%	7.44%	0.49%	0.00%
Wind=10	12.0	35.76%	20.46%	8.82%	2.07%	0.03%	0.00%
Wind=10	18.0	21.78%	9.43%	2.67%	0.30%	0.00%	0.00%
Wind=10	21.0	17.00%	6.40%	1.47%	0.12%	0.00%	0.00%
Wind=15	0.2	94.72%	93.81%	92.46%	90.17%	84.02%	64.39%
Wind=15	1.0	88.44%	84.28%	78.36%	69.13%	48.56%	12.84%
Wind=15	2.0	81.18%	73.71%	63.73%	49.59%	24.47%	1.71%
Wind=15	4.0	68.39%	56.38%	42.14%	25.52%	6.21%	0.03%
Wind=15	8.0	48.54%	32.99%	18.43%	6.76%	0.40%	0.00%
Wind=15	12.0	34.45%	19.30%	8.06%	1.79%	0.03%	0.00%
Wind=15	18.0	20.60%	8.64%	2.33%	0.24%	0.00%	0.00%
Wind=15	21.0	15.93%	5.78%	1.25%	0.09%	0.00%	0.00%
Wind=20	0.2	94.71%	93.79%	92.42%	90.11%	83.91%	64.16%
Wind=20	1.0	88.38%	84.18%	78.22%	68.92%	48.26%	12.61%
Wind=20	2.0	81.06%	73.53%	63.49%	49.30%	24.17%	1.65%
Wind=20	4.0	68.18%	56.11%	41.84%	25.22%	6.06%	0.03%
Wind=20	8.0	48.24%	32.68%	18.17%	6.60%	0.38%	0.00%
Wind=20	12.0	34.14%	19.03%	7.89%	1.73%	0.02%	0.00%
Wind=20	18.0	20.32%	8.46%	2.26%	0.23%	0.00%	0.00%
Wind=20	21.0	15.67%	5.64%	1.21%	0.08%	0.00%	0.00%

- TABLE A.6.a -

TRANSMITTANCE IN 3.5 UM BAND - STANDARD ATMOSPHERE PROFILE
*** LOWTRAN DATA ***

	Range in Km	Visibility in Kilometers 40	30	20	15	10	5
Wind=0	0.20	96.67%	96.64%	96.58%	96.52%	96.40%	96.05%
	1.00	90.27%	90.13%	89.86%	89.59%	89.05%	87.45%
	2.00	85.25%	84.99%	84.48%	83.97%	82.96%	80.01%
	4.00	77.78%	77.32%	76.40%	75.47%	73.67%	68.52%
	8.00	67.02%	66.22%	64.65%	63.09%	60.11%	52.01%
	12.00	58.64%	57.60%	55.55%	53.57%	49.81%	40.09%
	18.00	49.00%	47.70%	45.19%	42.78%	38.36%	27.70%
	21.00	45.01%	43.62%	40.95%	38.42%	33.82%	23.13%
Wind=5	0.20	95.61%	95.18%	94.32%	93.46%	91.78%	86.92%
	1.00	85.43%	83.53%	79.84%	76.28%	69.63%	53.06%
	2.00	76.35%	73.00%	66.68%	60.87%	50.73%	24.95%
	4.00	62.39%	57.04%	47.60%	39.66%	27.54%	9.29%
	8.00	43.12%	36.03%	25.10%	17.42%	8.40%	0.96%
	12.00	30.26%	23.12%	13.44%	7.77%	2.60%	0.10%
	18.00	18.17%	12.13%	5.37%	2.36%	0.46%	0.00%
	21.00	14.14%	8.83%	3.42%	1.31%	0.19%	0.00%
Wind=10	0.20	95.45%	94.96%	93.98%	93.01%	91.09%	85.61%
	1.00	84.72%	82.57%	78.42%	74.44%	67.09%	49.19%
	2.00	75.08%	71.33%	64.34%	57.97%	47.08%	25.31%
	4.00	60.34%	54.46%	44.30%	35.97%	23.73%	6.86%
	8.00	40.33%	32.86%	21.74%	14.33%	6.24%	0.52%
	12.00	27.37%	20.13%	10.84%	5.80%	1.66%	0.04%
	18.00	15.63%	9.86%	3.89%	1.52%	0.23%	0.00%
	21.00	11.87%	6.93%	2.34%	0.79%	0.09%	0.00%
Wind=15	0.20	95.40%	94.90%	93.90%	92.89%	90.92%	85.28%
	1.00	84.53%	82.33%	78.06%	73.97%	66.44%	48.23%
	2.00	74.76%	70.91%	63.74%	57.24%	46.18%	24.34%
	4.00	59.82%	53.82%	43.49%	35.07%	22.83%	6.34%
	8.00	39.64%	32.08%	20.95%	13.63%	5.77%	0.45%
	12.00	26.67%	19.42%	10.25%	5.38%	1.48%	0.03%
	18.00	15.03%	9.34%	3.58%	1.36%	0.20%	0.00%
	21.00	11.34%	6.51%	2.13%	0.69%	0.07%	0.00%
Wind=20	0.20	95.39%	94.88%	93.86%	92.84%	90.84%	85.12%
	1.00	84.45%	82.21%	77.89%	73.76%	66.15%	47.80%
	2.00	74.61%	70.71%	63.47%	56.91%	45.77%	23.90%
	4.00	59.58%	53.52%	43.12%	34.67%	22.43%	6.12%
	8.00	39.32%	31.73%	20.59%	13.31%	5.57%	0.41%
	12.00	26.36%	19.10%	9.99%	5.19%	1.41%	0.03%
	18.00	14.77%	9.11%	3.45%	1.29%	0.18%	0.00%
	21.00	11.10%	6.32%	2.03%	0.65%	0.07%	0.00%

- TABLE A.6.b -

TRANSMITTANCE IN 3.5 UM BAND - STANDARD ATMOSPHERE PROFILE
*** EMPIRICAL ***

Range in Km	Visibility in Kilometers 40	30	20	15	10	5
Wind= 0 0.2	91.41%	91.36%	91.35%	91.28%	91.12%	90.84%
Wind= 0 1.0	88.78%	88.53%	88.48%	88.13%	87.37%	86.06%
Wind= 0 2.0	85.59%	85.13%	85.02%	84.36%	82.91%	80.43%
Wind= 0 4.0	79.56%	78.70%	78.50%	77.28%	74.65%	70.26%
Wind= 0 8.0	68.73%	67.26%	66.92%	64.86%	60.52%	53.61%
Wind= 0 12.0	59.38%	57.48%	57.06%	54.44%	49.06%	40.90%
Wind= 0 18.0	47.69%	45.42%	44.91%	41.86%	35.81%	27.26%
Wind= 0 21.0	42.74%	40.37%	39.85%	36.70%	30.60%	22.26%
Wind= 5 0.2	90.45%	89.84%	88.86%	87.58%	84.55%	75.35%
Wind= 5 1.0	84.21%	81.41%	77.08%	71.67%	60.11%	33.78%
Wind= 5 2.0	77.01%	71.98%	64.53%	55.79%	39.23%	12.39%
Wind= 5 4.0	64.41%	56.26%	45.22%	33.80%	16.72%	1.67%
Wind= 5 8.0	45.06%	34.38%	22.20%	12.40%	3.04%	0.03%
Wind= 5 12.0	31.52%	21.01%	10.90%	4.55%	0.55%	0.00%
Wind= 5 18.0	18.44%	10.03%	3.75%	1.01%	0.04%	0.00%
Wind= 5 21.0	14.11%	6.93%	2.20%	0.48%	0.01%	0.00%
Wind=10 0.2	90.27%	89.60%	88.52%	87.10%	83.77%	73.72%
Wind=10 1.0	83.39%	80.33%	75.60%	69.74%	57.37%	30.28%
Wind=10 2.0	75.53%	70.07%	62.07%	52.82%	35.75%	9.96%
Wind=10 4.0	61.95%	53.32%	41.84%	30.30%	13.88%	1.08%
Wind=10 8.0	41.68%	30.88%	19.01%	9.97%	2.09%	0.01%
Wind=10 12.0	28.04%	17.88%	8.64%	3.28%	0.32%	0.00%
Wind=10 18.0	15.48%	7.88%	2.65%	0.62%	0.02%	0.00%
Wind=10 21.0	11.50%	5.23%	1.46%	0.27%	0.00%	0.00%
Wind=15 0.2	90.24%	89.55%	88.46%	87.01%	83.63%	73.42%
Wind=15 1.0	83.25%	80.13%	75.33%	69.39%	56.89%	29.68%
Wind=15 2.0	75.26%	69.73%	61.63%	52.29%	35.15%	9.57%
Wind=15 4.0	61.51%	52.80%	41.25%	29.70%	13.42%	0.99%
Wind=15 8.0	41.09%	30.28%	18.48%	9.58%	1.95%	0.01%
Wind=15 12.0	27.45%	17.36%	8.28%	3.09%	0.28%	0.00%
Wind=15 18.0	14.99%	7.54%	2.48%	0.57%	0.02%	0.00%
Wind=15 21.0	11.08%	4.97%	1.36%	0.24%	0.00%	0.00%
Wind=20 0.2	90.24%	89.55%	88.45%	87.00%	83.60%	73.37%
Wind=20 1.0	83.22%	80.09%	75.28%	69.33%	56.80%	29.57%
Wind=20 2.0	75.21%	69.67%	61.55%	52.20%	35.01%	9.50%
Wind=20 4.0	61.43%	52.71%	41.15%	29.59%	13.33%	0.98%
Wind=20 8.0	40.99%	30.17%	18.39%	9.51%	1.93%	0.01%
Wind=20 12.0	27.34%	17.27%	8.22%	3.06%	0.28%	0.00%
Wind=20 18.0	14.90%	7.48%	2.45%	0.56%	0.02%	0.00%
Wind=20 21.0	11.00%	4.92%	1.34%	0.24%	0.00%	0.00%

AD-A162 137 DEVELOPMENTS IN MODELLING THE USE OF INFRARED OFFBOARD COUNTERMEASURES IN AN INFRARED ANTI-SHIP MISSILE SCENARIO(U) NAVAL POSTGRADUATE SCHOOL MONTEREY CA 2/2

UNCLASSIFIED V D REED SEP 85 F/G 17/4 NL

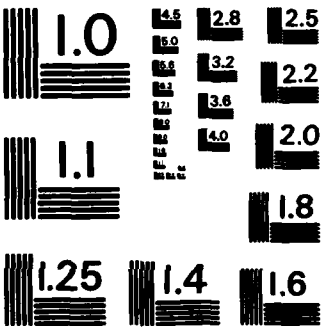

- TABLE A.7 -

TABLE OF A-COEFFICIENTS FOR SIX LOWTRAN PROFILES AT 3.5 um.

Tropical Profile

Visibility	40	30	20	15	10
Wind = 0	0.856781	0.856471	0.856390	0.856255	0.856115
Wind = 5	0.856363	0.856405	0.856220	0.857041	0.859499
Wind = 10	0.855773	0.856587	0.856102	0.855903	0.851515
Wind = 15	0.856526	0.856341	0.855761	0.856530	0.862983
Wind = 20	0.856982	0.857127	0.856171	0.857050	0.851565

Midlatitude Summer Profile

Visibility	40	30	20	15	10
Wind = 0	0.875788	0.875808	0.875754	0.875834	0.875812
Wind = 5	0.875747	0.875824	0.875699	0.875477	0.877011
Wind = 10	0.875820	0.875716	0.875650	0.874656	0.874052
Wind = 15	0.875753	0.875685	0.875366	0.876011	0.872420
Wind = 20	0.875777	0.875885	0.875886	0.877431	0.859462

Midlatitude Winter Profile

Visibility	40	30	20	15	10
Wind = 0	0.938293	0.938300	0.938272	0.938302	0.938302
Wind = 5	0.938338	0.938338	0.938284	0.937979	0.938643
Wind = 10	0.938264	0.938385	0.938206	0.937628	0.942839
Wind = 15	0.938298	0.938291	0.938232	0.939094	0.942642
Wind = 20	0.938236	0.938222	0.938328	0.937932	0.945244

- TABLE A.7 -

TABLE OF A-COEFFICIENTS FOR SIX LOWTRAN PROFILES AT 3.5 um.

Subarctic Summer Profile

Visibility	40	30	20	15	10
Wind = 0	0.900942	0.900967	0.900928	0.900916	0.900932
Wind = 5	0.900908	0.900991	0.900808	0.901004	0.897534
Wind = 10	0.900920	0.900967	0.901247	0.900275	0.910749
Wind = 15	0.900901	0.900910	0.901037	0.900193	0.903370
Wind = 20	0.901048	0.900953	0.900717	0.900709	0.889788

Subarctic Winter Profile

Visibility	40	30	20	15	10
Wind = 0	0.963535	0.963535	0.963587	0.963549	0.963600
Wind = 5	0.963548	0.963644	0.963652	0.963692	0.963209
Wind = 10	0.963594	0.963567	0.963533	0.963565	0.965684
Wind = 15	0.963558	0.963605	0.963507	0.963501	0.956474
Wind = 20	0.963587	0.963634	0.963474	0.963308	0.956391

U.S. Standard Atmosphere Profile

Visibility	40	30	20	15	10
Wind = 0	0.920811	0.920821	0.920850	0.920789	0.920866
Wind = 5	0.920841	0.920853	0.920746	0.920921	0.922365
Wind = 10	0.920800	0.920763	0.920945	0.920259	0.919745
Wind = 15	0.920802	0.920818	0.920675	0.920402	0.923306
Wind = 20	0.920836	0.920866	0.920934	0.920379	0.914907

- TABLE A.8 -

TABLE OF B-COEFFICIENTS FOR SIX LOWTRAN PROFILES AT 3.5 um.

Tropical Profile

Visibility	40	30	20	15	10
Wind = 0	-0.078300	-0.079883	-0.083265	-0.086652	-0.093444
Wind = 5	-0.132564	-0.154864	-0.199849	-0.245554	-0.337061
Wind = 10	-0.143678	-0.170376	-0.223794	-0.277764	-0.384270
Wind = 15	-0.146815	-0.174519	-0.230264	-0.286954	-0.401796
Wind = 20	-0.148416	-0.176768	-0.233486	-0.291292	-0.404436

Midlatitude Summer Profile

Visibility	40	30	20	15	10
Wind = 0	-0.064275	-0.065945	-0.069313	-0.072711	-0.079494
Wind = 5	-0.118579	-0.140899	-0.185840	-0.231112	-0.322254
Wind = 10	-0.129858	-0.156395	-0.209959	-0.263693	-0.371488
Wind = 15	-0.132919	-0.160663	-0.216479	-0.273163	-0.384626
Wind = 20	-0.134394	-0.162714	-0.219772	-0.277832	-0.386820

Midlatitude Winter Profile

Visibility	40	30	20	15	10
Wind = 0	-0.028635	-0.030311	-0.033691	-0.037106	-0.043922
Wind = 5	-0.082925	-0.105237	-0.150164	-0.195458	-0.286223
Wind = 10	-0.094293	-0.120931	-0.174555	-0.228508	-0.338264
Wind = 15	-0.097416	-0.125235	-0.181256	-0.238064	-0.352103
Wind = 20	-0.098874	-0.127235	-0.184428	-0.242007	-0.359376

- TABLE A.8 -

TABLE OF B-COEFFICIENTS FOR SIX LOWTRAN PROFILES AT 3.5 um.

Subarctic Summer Profile

Visibility	40	30	20	15	10
Wind = 0	-0.048863	-0.050536	-0.053881	-0.057260	-0.064021
Wind = 5	-0.103225	-0.125554	-0.170457	-0.215911	-0.305416
Wind = 10	-0.114354	-0.140914	-0.194472	-0.248144	-0.359279
Wind = 15	-0.117388	-0.145095	-0.201005	-0.257037	-0.370669
Wind = 20	-0.118852	-0.147091	-0.203899	-0.261375	-0.372554

Subarctic Winter Profile

Visibility	40	30	20	15	10
Wind = 0	-0.017768	-0.019474	-0.022912	-0.026375	-0.033305
Wind = 5	-0.071933	-0.094238	-0.139144	-0.184483	-0.274853
Wind = 10	-0.083740	-0.110510	-0.164416	-0.218868	-0.328210
Wind = 15	-0.087009	-0.115030	-0.171452	-0.228422	-0.340038
Wind = 20	-0.088548	-0.117162	-0.174745	-0.233146	-0.346934

U.S. Standard Atmosphere Profile

Visibility	40	30	20	15	10
Wind = 0	-0.036796	-0.038290	-0.041297	-0.044335	-0.050403
Wind = 5	-0.091927	-0.004360	-0.159548	-0.205238	-0.296848
Wind = 10	-0.100272	-0.125884	-0.177567	-0.229439	-0.333287
Wind = 15	-0.102441	-0.128875	-0.182099	-0.235793	-0.344040
Wind = 20	-0.103449	-0.130276	-0.184322	-0.238687	-0.345855

APPENDIX B

COMPUTER CODING TO INSTITUTE ATMOSPHERIC TRANSMITTANCE CALCULATION

The following FORTRAN code is designed to institute the calculation of atmospheric transmittance on an incremental range movement basis. As the missile closes its target(s) periodic recalculation of acquisition probabilities based on updated range and atmospheric transmittance are necessary to realistically model an engagement. Listed here are the subroutines necessary to calculate the transmittance based on the value of the current range value in the model. Although these subroutines are written in FORTRAN, they are simple and easily convertable to other languages. Comments regarding user alternatives are contained therein.

```
C     First thing to do is allow the user to select which
C     Atmospheric Profile is desired.  Then pass this to the
C     ATMOSP subroutine to calculate specific coefficients.
C     This input may be converted to disk-read input or
C     NAMELIST input if interactiveness is not desired.

      INTEGER ATPROF

      READ(111,*) ATPROF
  111 FORMAT(' Which Atmospheric Profile is desired ?'//
     1'    1.  Tropical'/
     2'    2.  Midlatitude Summer'/
     3'    3.  Midlatitude Winter'/
     4'    4.  Subarctic Summer'/
     5'    5.  Subarctic Winter'/
     6'    6.  U.S. Standard Atmosphere',I1)

      CALL ATMOSP(ATPROF)
```

```
C     The values of Wind and Visibility must already have
C     been input to the program prior to the above CALL.
C     ATMOSP calculates the 'A' and 'B' coefficients which
C     are necessary to refer to the TRANSM function.

      - - - - - - - - - - - - - -

      SUBROUTINE  ATMOSP(II)

      DIMENSION A1(6),A2(6),A3(6),A4(6),C1(6),C2(6),
     1          D1(6),D2(6),SIGMA(6)

      COMMON  ACOEFF,BCOEFF,VISIB,VWIND

      OPEN(UNIT=9,FILE='ATMPROF.DAT',STATUS='OLD')

      DO 1  I=1,6
         READ(9,*)  A1(I)
         READ(9,*)  A2(I)
         READ(9,*)  A3(I)
         READ(9,*)  A4(I)
         READ(9,*)  C1(I)
         READ(9,*)  C2(I)
         READ(9,*)  D1(I)
         READ(9,*)  D2(I)
         READ(9,*)  SIGMA(I)
    1 CONTINUE

      CLOSE(UNIT=9,STATUS='KEEP')

      ACOEFF = SIGMA(II)
      VCOEFF = A1(II) + A2(II)*VISIB + A3(II)*VISIB**2.
     # + A4(II)*VISIB**3.
      WCOEFF = 1. + D1(II)*(1.- EXP(D2(II)*VWIND))
      IF (VWIND.LE.0.1) THEN
          VWCOEF=1.0              !/* No correlation if
          GO TO 2                 !/* wind near zero.
      END IF
      VWCOEF = C1(II) * VISIB ** C2(II)
    2 BCOEFF = VCOEFF * WCOEFF * VWCOEF

      RETURN
      END

C     The two necessary coefficients (A or σ, B or α) are
C     computed and global for referencing by TRANSM for
C     transmittance calculation based on current range
C     values.  Now the function to perform equation 4.3.

      - - - - - - - - - - - - - -
```

```
      FUNCTION  TRANSM (RNG,AT)

C     The current range value is passed in as RNG, and AT is
C     the Atmospheric transmittance value passed back out.

      COMMON  RO,ACOEFF,BCOEFF

      AT = ACOEFF * EXP(BCOEFF*RNG)

      RETURN
      END
```

The file 'ATMPROF.DAT' referred to in subroutine ATMOSP above is an ASCII data file which contains all of the curve fitting coefficients listed in table 4.8. It is easily constructed with an editor, keeping in mind that if a name change is necessary, it must be performed in both places. The format is shown here and may be completed by referring to table 4.8. Ensure that no comments, blank lines or leading spaces occur when constructing the file.

```
-0.139154          !/*  Tropical        A1
6.2887E-03         !/*                  A2
-2.2354E-04        !/*                  A3
2.6091E-06         !/*                  A4
13.74105           !/*                  C1
-0.716806          !/*                  C2
0.895              !/*                  D1
-0.30              !/*                  D2
0.9383             !/*                   0
-0.1249852         !/*  Midlat Summer   A1
.                       .
 .                       .
  .                       .
   etc. for others in the order specified.
```

LIST OF REFERENCES

1. Kneizys, F. X., and others, Atmospheric Transmittance/Radiance: Computer Code LOWTRAN 6, Air Force Geophysics Laboratory (OPI), Hanscom AFB, 1983.

2. Hudson, Richard D. Jr., Infrared System Engineering, John Wiley and Sons, 1969.

3. Office of Naval Research, Handbook of Military Infrared Technology, U. S. Government Printing Office, 1965.

4. Schwartz, I. B., and others, Infrared Halo Effects Around Ships, Naval Research Laboratory Memorandum Report 5529, 29 March 1985.

BIBLIOGRAPHY

Boggs, R. B., Report of Changes to SIREM, Naval Research Laboratory Code 5700 Internal Report - Unpublished.

James, M. L., Smith, G. M., and Wolford, J. C., Applied Numerical Methods for Digital Computation, Harper and Row, 1977.

Lotus Development Corporation, Lotus 1-2-3 (TM), 1984.

Miller, I., and Freund, J. E., Probability and Statistics for Engineers, Prentice-Hall, 1985.

INITIAL DISTRIBUTION LIST

		No. Copies
1.	Defense Technical Information Center Cameron Station Alexandria, Virginia 22304-6145	2
2.	Library, Code 0142 Naval Postgraduate School Monterey, California 93943-5100	2
3.	Naval Research Laboratory Attn: Code 5700 Ed Powell Washington, D. C. 20375	2
4.	Commander, Space and Naval Warfare Systems Command Attn: PDW-107-5E Washington, D.C. 20363-5100	1
5.	President, Naval War College Attn: EW Chair Newport, Rhode Island 02841	1
6.	Superintendent, Naval Postgraduate School Attn: Professor A. W. Cooper (Code 61Cr) Monterey, California 93943	2

END

FILMED

1-86

DTIC